New Insights into the South American Low Level Jet from RELAMPAGO Observations

Clayton Robert Stanley Sasaki

A thesis

submitted in partial fulfillment of the

requirements for the degree of

Master of Science

University of Washington

2021

Committee:

Lynn McMurdie

Angela Rowe

Shuyi Chen

Alexandra Anderson-Frey

Program Authorized to Offer Degree:

Atmospheric Sciences

University of Washington

Abstract

New Insights into the South American Low Level Jet from RELAMPAGO Observations

Clayton Robert Stanley Sasaki

Co-Chairs of the Supervisory Committee:
Lynn McMurdie and Angela Rowe
Department of Atmospheric Sciences

The Remote sensing of Electrification, Lightning, And Mesoscale/microscale Processes with Adaptive Ground Observations (RELAMPAGO) campaign produced unparalleled observations of the South American Low-Level Jet (SALLJ) in Central Argentina with high temporal observations located in the path of the jet and near rapidly growing convection. The vertical and temporal structure of the jet is characterized using 3-hourly soundings launched at two fixed sites near the Sierras de Cordoba (SDC), along with high-resolution reanalysis data. Objective SALLJ identification criteria are applied to each sounding to determine the presence, timing, and vertical characteristics of the jet. The observations largely confirm prior results showing that low-level jets (LLJs) most frequently come from the north, occur overnight, and peak in the low levels, though LLJs notably peaked higher near the end of longer duration events during RELAMPAGO. This study categorizes LLJs into short-lived events that appear to follow a diurnal cycle and long-lived events that are more elevated and lack a clear diurnal cycle. All observed LLJs appeared to be, at least partially, synoptically driven with evidence of subsynoptic scale processes clearer in the short-lived events. Importantly, evidence of both boundary layer processes and large-scale forcing were observed during short-lived cases, but in long-lived cases,

the synoptic forcing was dominant. Lastly, higher levels of moisture and larger convective coverage east of the SDC occurred near the end of the long-lived LLJ periods.

TABLE OF CONTENTS

LIST OF FIGURES

LIST OF TABLES

AKNOWLEDGEMENTS

I would like to thank my co-advisors, Angela Rowe and Lynn McMurdie, for their continued support, exceptional mentorship, and infectious enthusiasm. I also appreciate the guidance from my thesis committee – Lynn McMurdie, Angela Rowe, Shuyi Chen, and Alexandra Anderson-Frey – and thank them for helpful discussions and feedback related to this project. Funding support for this research came from the National Science Foundation (AGS 1661768). I would also like to thank the Achievement Rewards for College Students for not only supporting me financially but being such a supportive community.

I am grateful for the other faculty, staff, postdocs, and students as this department would not be what it is without the warm, friendly, and supportive nature of all of its members. In particular, I would like to thank my cohort – Yuk Chun Chan, Tyler Cox, Andrew DeLaFrance, Carley Fredrickson, Lily Hahn, Daniel Lloveras, Jacqueline Nugent, Phil Rund, Greta Shum, Adam Sokol, Lindsey Taylor, Sami Turbeville, Mingcheng Wang, Claire Zarakas – their friendship has been invaluable.

Finally, I am thankful to my parents, sister, and fiancée, Kayla. Their unwavering support and ability to listen to me talk through my research has been crucial for my success.

Chapter 1.
INTRODUCTION

Some of the most intense convective storms in the world are located east of the Andes in Central Argentina (Zipser et al. 2006; Houze et al. 2015; Liu and Zipser 2016). Convective systems in this region have a duality of impacts. They provide the water supply that supports the population as well as the extensive agriculture industry, including major wine-producing regions, and produce greater than 90% of the rain in Southeastern South America (Nesbitt et al. 2006; Rasmussen et al. 2016). Yet, at the same time, baseball-size hail, flooding rains, and frequent lightning create a major hazard for the people and crops in the region (Zipser et al. 2006; Rasmussen et al. 2014). Understanding how storms organize and grow into larger mesoscale systems can help with prediction of these high-impact weather events.

Previous modeling and satellite studies in Central Argentina have emphasized the South American Low-Level Jet (SALLJ) as a recurring feature around the time of development of mesoscale convective systems (MCSs; Nicolini and Saulo 2000; Salio et al. 2002; Salio et al. 2006; Borque et al. 2010; Rasmussen and Houze 2016). The SALLJ is a ribbon of fast-moving air in the lower levels of the atmosphere, oriented mostly north-south, that lies east of the Andes (blue arrow Fig. 1) and transports moisture-laden air from the tropics to the midlatitudes (Rasmusson and Mo 1996; Nogues-Paegle and Mo 1997; Nascimento et al 2016). Additionally, it has been hypothesized that the SALLJ episodes reaching farther south into Central Argentina create favorable thermodynamic and dynamic conditions for convection beyond moistening the environment. These influences include increasing low-level convergence, wind shear, and persistent horizontal advection of heat (Salio et al. 2007; Saulo et al. 2007). Detailed knowledge of the characteristics and variability of the SALLJ are needed to further our understanding of the

relationship between the SALLJ and MCSs, which could be critical to predicting MCS development and maintenance (Carril et al. 2012; Anabor et al. 2008).

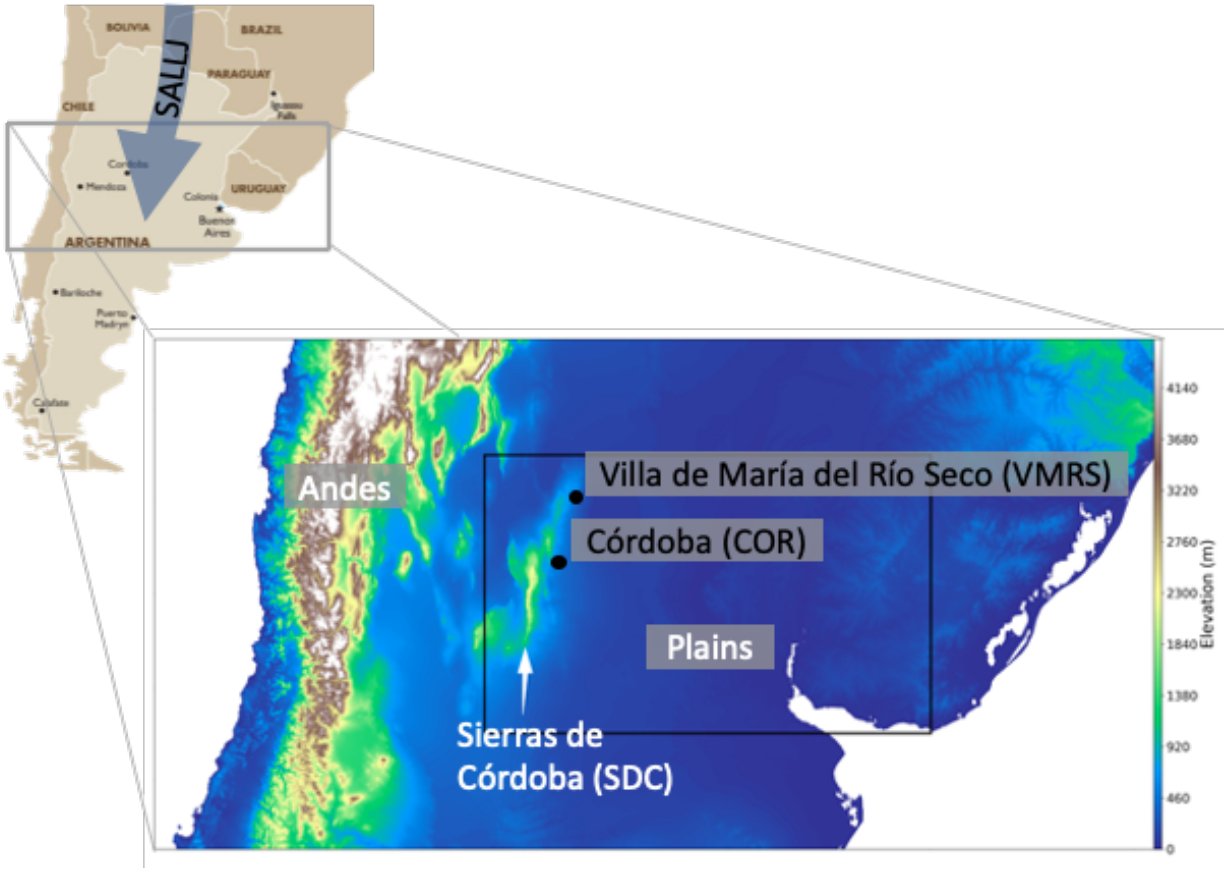

Figure 1: Map depicting the general RELAMPAGO study area including the Sierras de Córdoba region (black outline), two fixed sounding sites (black text), the SALLJ (blue arrow), and elevation (color shading) with notable topographic features (white text). The two soundings sites used in this study are Córdoba and Villa de Maria del Rio Seco.

Past work, largely from a U.S. perspective, has linked low-level jets (LLJs) to many atmospheric mechanisms, but broadly classified them into two types: nocturnal and synoptically-related LLJs (e.g., Stensrud 1996). Nocturnal LLJs (NLLJs) are associated with boundary layer processes such as inertial oscillations and shallow baroclinic processes. They have a wind maximum within the planetary boundary layer and their intensity often follows a clear diurnal cycle, peaking overnight (Blackadar 1957; Holton 1967; Bonner 1968; Shapiro et al. 2016). A second type is synoptically-related LLJs, termed by some as low-level jet streams (LLJS;

Stensrud 1996), which result from tight pressure gradients in synoptic systems and are often linked to upper level jet streaks via ageostrophic transverse circulations. These LLJs tend to be more elevated, have a larger vertical extent compared to NLLJs, and often lack clear diurnal cycles (Hoecker 1963; Uccellini 1980; Chen et al. 1994; Du et al. 2012, 2014). Characteristics of both types of LLJs have been documented in the context of the SALLJ (Salio et al. 2002; Nicolini et al. 2004; Rife et al. 2010; Repinaldo et al. 2014; Oliveira et al. 2018), but the specific mechanisms are still not well understood owing, in part, to a lack of routine high spatially and temporally resolved ground and upper-air observations in the path of the jet.

The first extensive observations of the SALLJ came from the South American Low-Level Jet Experiment (SALLJEX; Vera et al. 2006), which included observations from an upper-air network and aircraft from early January to mid-February 2003. The project was centered in Bolivia where the peak winds of the SALLJ are thought to occur (Byerle and Paegle 2002; Salio et al. 2002; Campetella and Vera 2002; Silvers and Schubert 2012). These observations documented an overnight peak in LLJ intensity; however, despite improvements in temporal resolution (soundings up to 4 times daily) the exact timing of the peak LLJ could not be resolved. A summertime low-level wind gyre was also found within the SALLJEX study region with a clearer wind rotation when a LLJ was present. These SALLJEX findings linked the jet timing to a combination of an inertial oscillation, a subsynoptic pressure gradient related to mountain-valley differential diurnal heating, and a dominant meridional mean wind (Nicolini et al. 2004; Vera et al. 2006). Prior research, stemming from SALLJEX observations, has emphasized small scale processes that produce the mean SALLJ profiles. While this research has focused predominantly on LLJs that peak below 850 hPa, jets with speed maximums as high as 3 km were also noted.

Besides SALLJEX, most of our knowledge of the SALLJ in Central Argentina comes from reanalysis, modeling, and satellite studies. Multiple reanalysis studies found that the majority of LLJs in this region do peak below 1500 m or about 850 hPa (Salio et al. 2002; Rife et al. 2010; Oliveira et al. 2018; Montini et al. 2019). However, Oliveira et al. 2018 (hereafter ONK18) found a significant number of more elevated jets. They determined that strong site-to-site variability in SALLJ heights, across Southeastern South America, motivated the need for LLJ identification methods that were localized. ONK18 created more flexible criteria than was previously applied (Bonner 1968; Nicolini and Saulo 2000; Salio et al. 2002) by searching height ranges rather than specific pressure levels (e.g., 850 and 700 hPa in Nicolini and Saulo 2000), deepening the layer for LLJ identification, and dropping a weak zonal component requirement. These criteria allowed more LLJ days to be captured throughout South America than previous studies (ONK18 Figs. 3 and 6), including more instances of elevated SALLJs with strong zonal components. They hypothesized that the propensity for elevated LLJs was related to synoptic-scale baroclinic systems, but emphasized the need for additional studies on the patterns and forcing mechanisms controlling the elevated LLJs in Southeastern South America.

Modeling studies have emphasized synoptic environments that might contribute to the presence of the SALLJ in Central Argentina. The subset of jets that extend past 25°S into Northern Argentina are called Chaco low-level jets (Nicolini and Saulo 2000; Salio et al. 2002; Nicolini et al. 2004b). These jets have been linked to the deepening of the thermo-orographic Northwest Argentina Low (NAL), which may help to lengthen the meridional flow and extend the jet down into Argentina. The NAL is a semi-permanent feature during the summer due to strong surface warming, but orographic subsidence linked to transient activity modulates its intensity (Seluchi et al. 2003). Strong lee cyclogenesis has been found to occur ahead of upper-

level troughs traversing the Andes (Rasmussen and Houze 2016) and could be partially responsible for strengthening the NAL and therefore enhancing the SALLJ. Unlike NLLJs driven by boundary layer processes, this intensification of the gradient due to lee cyclogenesis does not necessarily weaken during the day and could be responsible for the extension of the LLJ beyond the PBL (Uccellini 1980; Saulo et al. 2004). Additionally, the importance of the Atlantic High, located to the east of the LLJ, in strengthening the pressure gradient associated with the LLJ is not well understood. During SALLJ events present in this large-scale environment, most of the convective activity was hypothesized to occur over central and eastern Argentina, southern Brazil, and Uruguay (Salio et al. 2002; Nicolini et al. 2002; Nicolini et al. 2004b). Salio et al. (2002) found that these jet events lasted 1-10 days, although less frequently in longer durations. Past work has provided hypotheses for drivers of the SALLJ from boundary layer processes to synoptic gradients, but limited observations have failed to deduce the relative importance of these processes to various SALLJ episodes. Increased observations of the SALLJ will help to connect characteristics of the SALLJ to the various hypothesized drivers.

The Remote sensing of Electrification, Lightning, And Mesoscale/microscale Processes with Adaptive Ground Observations (RELAMPAGO; Nesbitt et al. 2021) project took place in late 2018 in Central Argentina, deploying a broad array of instrumentation including soundings in the path of the SALLJ up to every 3 hours around forecasted convectively active periods. The main period of the campaign was from 1 November to 17 December 2018, focusing earlier in the convective season and farther south than SALLJEX. The study region of RELAMPAGO in Central Argentina lies in an area that is a maximum in LLJ days (Nicolini and Saulo 2000; Oliveira et al. 2018), often near the terminus of the SALLJ (Paegle 1998; Salio et al. 2002), and where the SALLJ coincides with the Sierras de Córdoba (SDC), a mesoscale mountain range east

of the Andes that is a focal point for convective initiation and rapid upscale growth to MCSs (Rasmussen et al. 2014; Mulholland et al. 2018). It has been hypothesized that the modification of the SALLJ by the SDC could partially explain the frequent convective initiation and upscale growth into MCSs in this region (Rasmussen and Houze 2016).

This study presents an observational analysis of the SALLJ during the RELAMPAGO campaign (late spring/early summer Central Argentina) using frequent soundings from two fixed stations in the path of the jet, providing an unprecedented characterization (e.g., timing, peak speed, direction, height) of the SALLJ near the SDC. Reanalysis data are then used to fill in spatial and temporal observational gaps and to expand on the thermodynamic influences of the SALLJ. This detailed analysis of the SALLJ during varying synoptic scale environments allows for links between environments on many scales and characteristics of the SALLJ. To our knowledge, this study presents the first look at the SALLJ near the SDC using high temporal observational data. Additionally, the recently released ERA5 has higher temporal and spatial resolution than past reanalysis data used for LLJ studies in this region. The objectives of this study are to: 1) Develop objective criteria for identifying the SALLJ near the SDC; 2) Describe the variability in the vertical and temporal structure of the SALLJ observed during RELAMPAGO; 3) Link variability in jet height and duration to synoptic and subsynoptic features; and 4) Investigate moisture transport and the presence of convection during periods of SALLJ activity.

Chapter 2.
DATA & METHODS

2.1 Fixed soundings

Throughout the RELAMPAGO period (1 November - 17 December 2018), soundings were launched at two fixed sites positioned in the path of the jet (Fig. 1): Córdoba (COR; 31.298°S, 64.212°W; elevation 490 m) and Villa de María del Río Seco (VMRS; 29.906°S, 63.726°W; elevation 341 m). The operational COR site lies just to the east of the SDC, and the sounding frequency was increased for RELAMPAGO to characterize the near-convective environment. The VMRS site is farther north and is unique to RELAMPAGO. VMRS was selected specifically to monitor the SALLJ and therefore sounding launches were heavily weighted towards periods of expected LLJ activity. The default launch frequency during the campaign was two times per day (0000 and 1200 UTC) at COR and once a day (0900 UTC) at VMRS. Three-hourly soundings (i.e., 8 per day) were launched during intense observation periods (IOPs), with two short periods of hourly soundings at COR and one at VMRS. A total of 175 and 136 soundings were launched at COR and VMRS, respectively (Table 1). About three-quarters of the soundings at both stations were launched during the IOPs, but there is a clear bias towards default launch times: around half of the soundings at COR and a third at VMRS were launched at those times. The winds from these soundings were used to identify LLJs and their characteristics (e.g., timing, peak speed, direction, height). The sounding sites were operated by the Servicio Meteorológico Nacional (SMN) and all radiosondes used were Modem GPSonde M10 with 2-s vertical resolution (Servicio Meteorológico Nacional-Argentina 2019).

	Total Soundings	Number of LLJs Identified		
		Oliveira et al. 2018 Criteria	Modified Criteria	Percent increase in LLJ
COR	175	60 (34.3)	67 (38.3)	11.7%
VMRS	136	81 (59.6)	89 (65.4)	9.9%

Table 1: Number of soundings with LLJs identified (percentage of total launched) at COR and VMRS for both the Oliveira et al. (2018) criteria and our modified criteria.

Two types of automated data quality checks (gross limit and rate of change checks) and a manual visual examination were carried out by NCAR/EOL Processing and Quality Control (UCAR/NCAR-Earth Observing Laboratory 2020). Additionally, low-level winds in LLJ soundings were examined for convection contamination. First, a qualitative inspection was conducted using saturated layers in the soundings and GOES-16 IR brightness temperatures to determine the presence of convection. Using this method, about one-fifth of the soundings had clouds present, but only a handful were identified as in convection. Convection did not appear to affect the low-level winds in any of the soundings, but three soundings within deep convection extending from the low levels on 12 November at VMRS were not included in the statistics out of caution.

2.2 Identification of LLJs

The criteria used in this study to identify the SALLJ during the RELAMPAGO campaign are based on ONK18's method. A LLJ was identified by ONK18 when 1) Winds displayed a local maximum in speed within the lowest 3000 m AGL and the maximum was equal or greater than 12 m s^{-1}, and 2) The wind speed decreased by at least 6 m s^{-1} from the maximum speed to the first minimum found aloft or to the speed at 4000 m AGL, whichever occurred first. While the

ONK18 criteria captured elevated jets better than past criteria, it could not identify LLJs during widespread convective events during RELAMPAGO when the jet was broader and elevated. For example, the ONK18 criteria failed to identify a SALLJ in the 1200 UTC 12 November and 0900 UTC 13 December observational soundings at COR (Fig. 2) due to the deep layer of strong winds. Therefore, modifications were made to the ONK18 criteria to capture broader and more elevated LLJs observed in the RELAMPAGO sounding dataset by deepening the layers over which to search for the wind minimum aloft and for the wind maximum, respectively. A RELAMPAGO wind profile therefore must meet the following two criteria to be considered a LLJ:

- Winds must display a local maximum in speed within the lowest 3200 m AGL and the maximum must be equal to or greater than 12 m s^{-1} (23.33 kts).
- The wind speed must decrease by at least 6 m s^{-1} (11.66 kts) from the maximum speed to the first minimum found aloft or to the speed at 5700 m AGL, whichever occurs first.

By allowing the minimum to be found higher, we capture the true minimum in both cases shown in Figure 2. Additionally, the combination of the two modifications captures the true maximum and minimum for the 0900 UTC 13 December sounding which allows it to be classified as a LLJ. The hierarchy established in ONK18 for dual-core or wide-core LLJs has been preserved in that the strongest and lowest jet core is classified as the LLJ in these scenarios. The modified criteria better identify persistent and elevated jets that bring significant moistening to the lower levels and are associated with times of widespread convection in this region, as will be shown in the results section below.

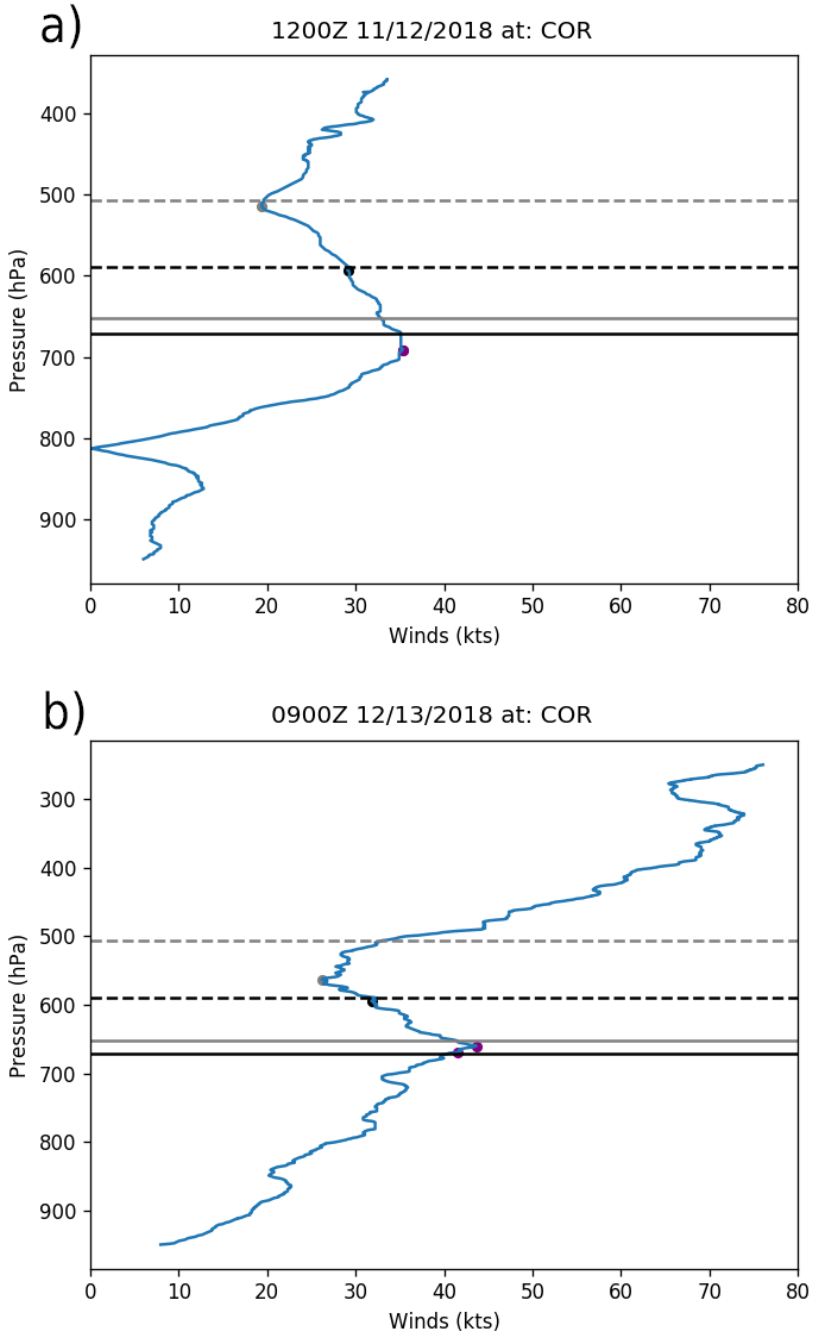

Figure 2: Example vertical wind profiles from COR soundings showing application of the LLJ identification criteria: maximum wind (purple dot), minimum found by Oliveira et al. 2018 criteria (black) and minimum found by the modified criteria used in this study (gray). The lines mark the top of the search areas for wind maxima (solid) and minima (dashed lines) for the two criteria.

2.3 European Centre for Medium-Range Weather Forecasts Reanalysis (ERA5)

ERA5 is the fifth generation of atmospheric reanalysis produced by the European Centre for Medium-Range Weather Forecasts (ECMWF; Hersbach et al. 2020). It has hourly output and a horizontal resolution of 31 km on 37 pressure levels. In the low-to-mid levels, the interval of pressure levels is 25 hPa from 1000 to 750 hPa and 50 hPa from 750 to 450 hPa. Compared to past reanalysis datasets that covered this region (e.g., Climate Forecast System Reanalysis, older versions of ERA), ERA5 has increased temporal and spatial resolution. ERA5 hourly winds, heights, and specific humidity are used in this study to supplement the fixed soundings launched during RELAMPAGO and put the observations in a broader spatial and temporal context. From our investigation (Appendix A), the evolution of synoptic-scale ERA5 wind patterns and moisture transport appear to be adequate for addressing this study's objectives. However, additional comparisons should be carried out to determine if ERA5 is suitable for more targeted, case study-based LLJ analysis. Due to this limitation, periods of northerly flow are identified in ERA5 data but ERA5 data is not used to objectively identify the LLJ at specific times. The ERA5 analysis in this study is conducted within the following domains: South America (5°N-55°S, 35°-95°W) for the synoptic maps, and the geographical domain of the SALLJ (10°-50°S, 55°-65°W) for the Hovmöller diagrams.

2.4 Geostationary Operational Environmental Satellite R-series (GOES-R)

GOES-16 IR brightness temperatures with a horizontal resolution of 2 km and temporal resolution of 15 minutes were used to determine spatial coverage of convection throughout the campaign. A threshold of 235 K was used within the box defined by 29-35°S, 55-65°W (black box Fig. 1). This area is downstream of the SDC and close to the terminus of the SALLJ. The brightness temperature threshold of 235 K was used as it was determined to be suitable for detecting clouds associated with convection in different regions of South America (Vila et al. 2008; Carvalho and Jones 2001).

Chapter 3.
RESULTS

3.1 Variability in the SALLJ

The number of LLJs found during RELAMPAGO using the ONK18 criteria and our modified criteria is shown in Table 1. A higher percentage of soundings had LLJs identified at VMRS than at COR; however, the difference between the two stations is likely an artifact of when soundings were launched at the two stations (i.e., preferential launches at VMRS during forecasted LLJ periods). The modified criteria resulted in about 4-6 % more soundings containing LLJs than using ONK18 (an ~10-12% increase in LLJs), but more important to this analysis are the times when these additional LLJs were identified. Time series of the v-component of the wind from soundings launched during RELAMPAGO at COR and VMRS are shown in Figures 3 and 4, where red indicates northerlies and blue, southerlies. The height of maximum wind (jet core) is indicated for soundings with LLJs defined by the ONK18 criteria (black squares) and those added when using the more relaxed modified criteria described in the Methods section (gray x's). During RELAMPAGO, northerly flow varied in duration and depth. The majority of periods of strong northerly winds lasted for 2 days or less; however, there were two longer duration periods (~5-6 days), 8-12 November and 8-13 December (black boxes in Fig. 3 and 4). Overall, the jet core winds were below 750 hPa, but more elevated and broader northerly LLJs were captured using the modified criteria (~700 hPa; gray circles), primarily during the longer duration periods. Widespread convective events near the SDC were also observed near the end of these same long-duration jet periods (e.g., Piersante et al. 2021). The modified criteria will therefore hereafter be used to characterize the LLJ in this study.

Figures 5 to 7 provide objective quantifications of the variations in direction, speed, height, and timing of the SALLJ. Beginning with wind direction, Figure 5 shows that the majority of LLJs were found to be from a northerly direction (between NW and NE) at both stations and specifically all elevated jets are from a northerly direction (gray x's Figs. 3 and 4). Jets from the NNW are more common at VMRS than COR and the percentage from the NNW at COR is even further reduced when elevated and broader LLJs are removed (not shown). These results combined indicate that low-level winds are likely blocked at COR to the west due to the higher terrain of the SDC (seen in Fig. 1).

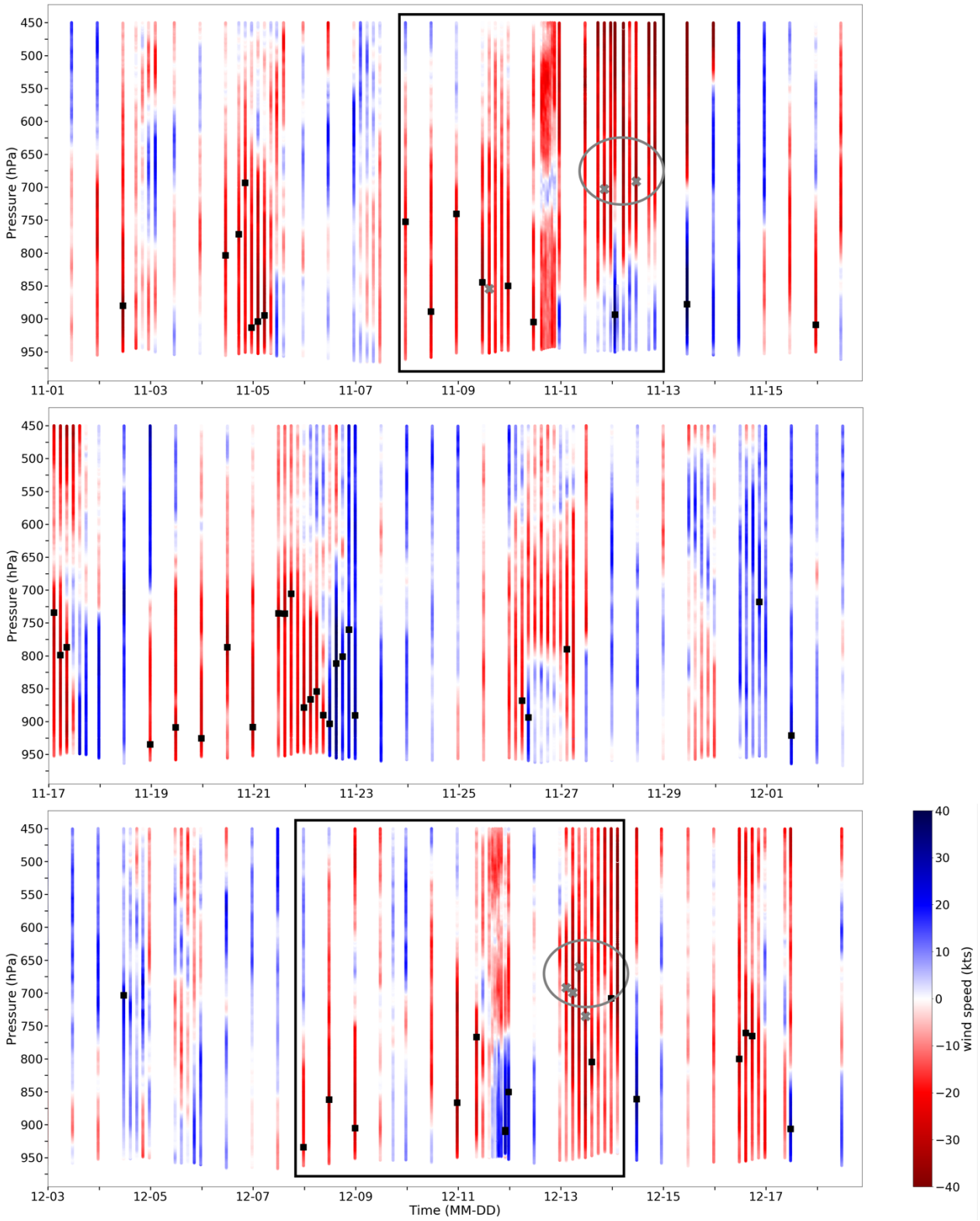

Figure 3: Time series of soundings launched during the RELAMPAGO campaign at COR with the v-component of the wind from the north (red) and from the south (blue). The arrows point to the level of maximum wind (jet core) for soundings with a LLJ identified from Oliveira et al. (2018) criteria (black squares) and additional LLJs found when applying our modified criteria (gray x).

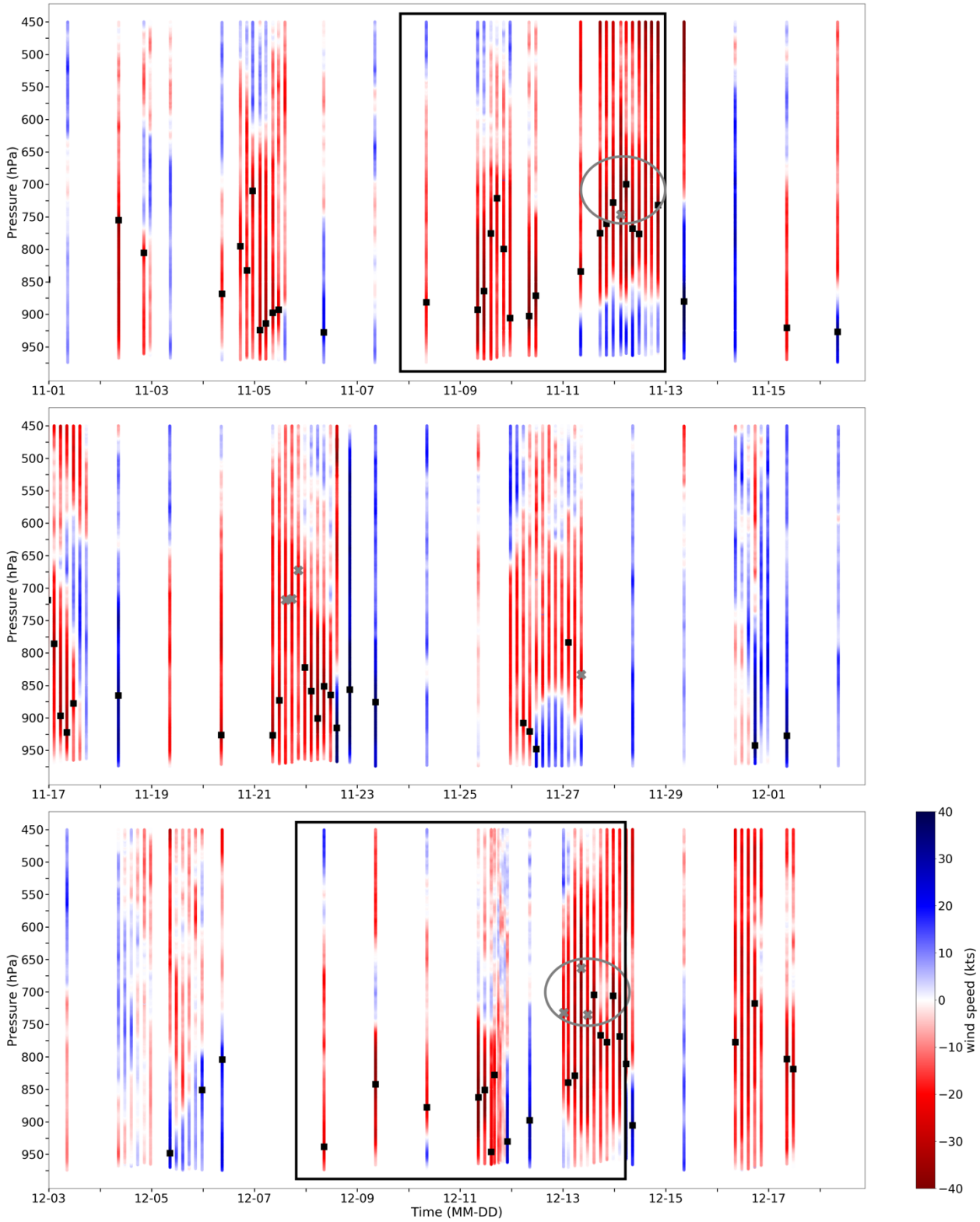

Figure 4: Same as Figure 3 but for VMRS.

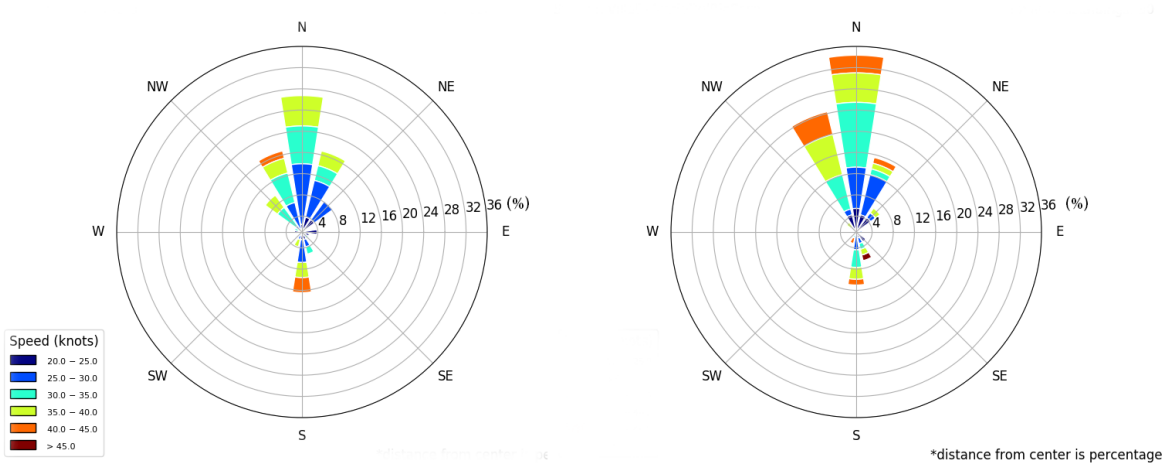

Figure 5: Wind roses showing the percentage of all LLJ soundings with a specific wind direction and wind speed (color shading) at jet core height using the modified criteria at COR (left) and VMRS (right).

In general, stronger LLJs were observed more often at VMRS than COR (Fig. 5 and right panels in Fig. 6). Maximum wind speeds were skewed toward weaker winds at COR with a median of 29 kts, while at VMRS the distribution of maximum winds was more uniform and had a median of 32 kts. A comparison of LLJ core wind speeds when the jet was observed at both stations at the same time verified that VMRS often tended to have higher max wind speeds than COR. This agrees with past modeling work that found winds increasing north to a peak in Bolivia/Paraguay (Byerle and Paegle 2002; Salio et al. 2002; Campetella and Vera 2002; Silvers and Schubert 2012). However, elevated and broader LLJs tended to be more similar in intensity at the two stations (not shown).

In terms of the level of maximum wind, both stations have a greater frequency of LLJs in the lower levels with this being particularly evident at COR (left panels in Fig. 6). At both stations about half of the LLJs peaked in the lowest 100 hPa (from 950 to 850 hPa) with the other half peaking above 850 hPa. Notably, jet cores were found up to 650 hPa. With a once daily 15-year dataset, ONK18 found that about 20-25% of jets in Southeastern South America displayed a core above 1500 m (~850 hPa) and, focusing on northerly LLJs at COR, ONK18

found a higher percentage (39%) of jet cores above 1500 m. The increased percentage of elevated jets in the SDC region, as compared to previous studies, could be a result of our higher temporal analysis or due to our focus on spring/early summer.

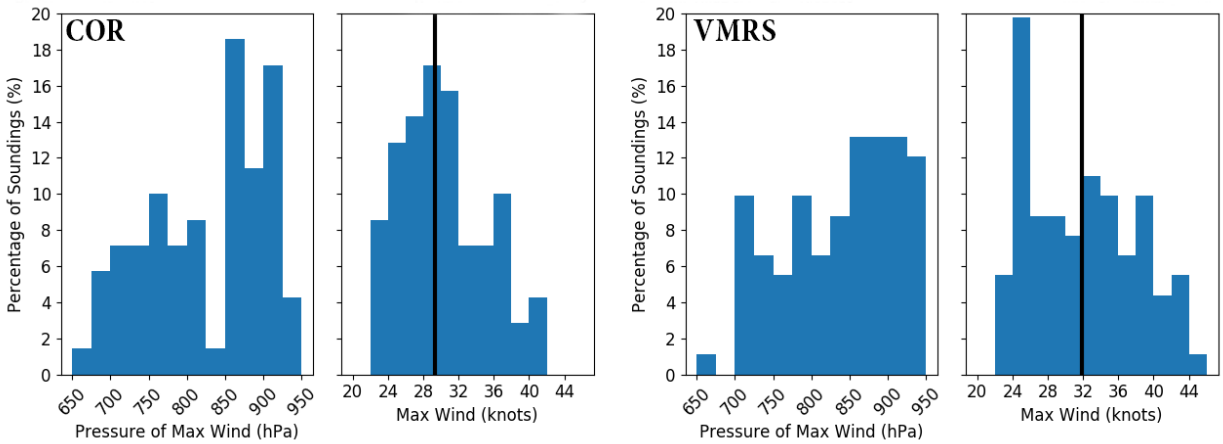

Figure 6: The distribution of jet core wind speeds and the pressure levels where they occurred for all LLJs at COR (left) and VMRS (right). The black lines are median jet core wind speeds.

A key difference between NLLJs and LLJS is the presence of diurnal cycles (e.g., Stensrud 1996); therefore, the timing of when LLJs are identified can provide insight into the atmospheric phenomena driving the SALLJ. As mentioned in the introduction, NLLJs are known to be more frequent and intense overnight, whereas LLJS do not follow this diurnal cycle. For the remainder of this study, we will focus on northerly LLJs. Figure 7 shows that the highest percentage of LLJ soundings occurred overnight into the early morning (between 0300-1200 UTC) with the lowest percentage during the afternoon (1500-1800 UTC). For this analysis the bias of when soundings were launched had to be removed. For example, more soundings were launched at 0000 and 1200 UTC than other times for COR and at 0900 UTC for VMRS because those were operational times that had consistent launches. This launch bias was reduced by focusing only on days with enough soundings to fully represent the diurnal cycle, meaning 7-8 3-hourly soundings had to be available in a 24-hr period for those soundings to be included in the analysis. Unfortunately, only about a third to a half of the soundings were in periods that met this

definition, covering about a fifth of the 45-day campaign. This finding of a diurnal cycle in LLJ identification is consistent with past studies that have found that LLJs follow a clear diurnal cycle and confirms, from a broad sense, the influence of diurnal processes (Salio et al. 2002; Nicolini et al. 2004; Marengo et al. 2004).

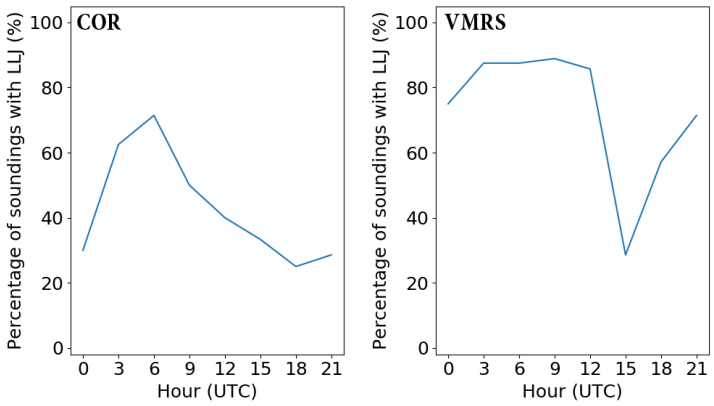

Figure 7: Percentage of soundings at each hour with northerly LLJs identified for COR (left) and VMRS (right). Note: local time is UTC-3

From the observational soundings (Figs. 3 and 4), SALLJ episodes of varying duration were identified, but, due to gaps in observations, it was difficult to clearly determine duration. ERA5 is used to gain a more complete picture of the duration of northerly flow events. Figure 8 is a north-south Hovmöller diagram of ERA5 850-hPa v-wind where the y-axis is latitude, showing the spatial and temporal extent of enhanced northerly flow events at various latitudes. The hourly data provided by ERA5 further elucidates the northerly LLJ episodes identified in COR and VMRS observations. Six periods of northerly low-level flow that exist for 1-2 days (gray circles) are visible along with the two longer 5-6 day time periods (black boxes). While the two periods of longer-duration northerly flow are of similar length, they have quite different flow patterns. From 8-12 November continuous northerly flow was present, while three pulses of northerly wind bursts were seen during the 8-13 December period. It is important to note that

Figure 8 highlights periods of northerly/southerly flow and does not distinguish times when a LLJ was identified within them. As stated above, a more detailed analysis must be done to evaluate how well ERA5 objectively captures the SALLJ on a case-study basis.

Overall, RELAMPAGO observations mostly confirmed characteristics of the SALLJ in Central Argentina inferred from previous reanalysis and modeling studies in that the majority of the LLJs are from the north, peak in the lower levels, occur overnight, and are present for less than two days. However, there are two longer duration events with observed elevated LLJs near the end of each of these two periods which warrant closer study in linking jet characteristics to the conditions under which they form.

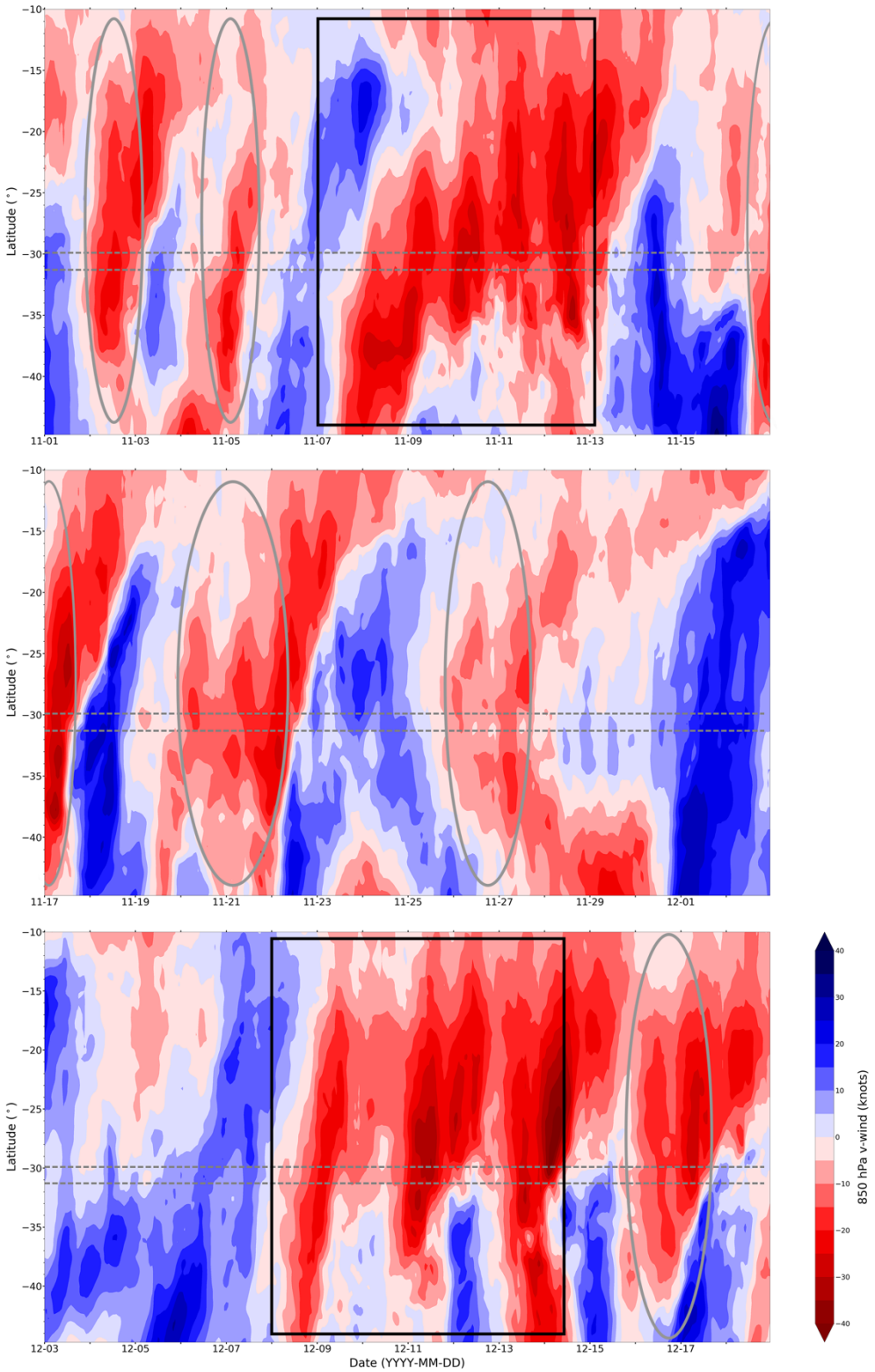

Figure 8: N-S Hovmöller diagram of the v-component of the wind at 850 hPa averaged over -55° to -65° W using ECMWF Reanalysis 5 (ERA5). Red is wind from the north and blue is wind from the south. Dash-dot lines show the latitude of VMRS (upper) and COR (lower). Instances where a northerly LLJ is seen in Central Argentina are highlighted. The black boxes are the two extended northerly LLJ events from the observational plots and the gray circles are shorter lived LLJ events.

3.2 Comparison of short-lived vs. long-lived SALLJs

3.2.1 Characteristics

Based on the observational and ERA5 time series (Figs. 3, 4, and 8), those SALLJ events that lasted for less than 2 days were classified as short-lived SALLJs and those that lasted more than 2 days as long-lived events. Comparing the characteristics and synoptic set up of the short- and long-lived jet cases can provide insight into the mechanisms that control the SALLJ in the region, including the duration, timing, and height of these northerly jets.

To explore the evolution of the SALLJ in these cases in more detail, the v-wind component was plotted from soundings at COR on days when more than six 3-hourly soundings were available and a LLJ was present (Fig. 9). COR is shown because more soundings are available, but similar conclusions can be drawn at VMRS and any important differences will be highlighted. Using this previously explained requirement for sounding days, four short-lived LLJ events were identified during RELAMPAGO. However, this study is limited by the number of days with high temporal soundings and from Figure 8 this type of SALLJ (i.e., strong northerly flow persisting for less than 2 days) occurred six times. The general characteristics are similar across all of these events and are represented by the 5 November soundings (Fig. 9a). These short-lived jet-period characteristics are: 1) duration 1-2 days (by definition), 2) V-component of the jet strongest overnight/early morning (red circle), 3) jet core below 800 hPa, and 4) a switch to southerly low-level winds after the northerly LLJ weakens (blue circle). At VMRS the short-lived LLJs displayed similar characteristics, but the diurnal cycle was shifted a couple hours later and southerly winds were weaker in the afternoon. Most of the characteristics resemble those of NLLJs; however the switch in the low-level wind to southerly appears to be related to synoptic scale drivers and possible frontal boundaries. The delay in this switch to the south between COR

and VMRS is consistent with a frontal boundary moving up from the south and will be discussed in a later section.

The two long-lived LLJ events (> 2 days in duration) did not exhibit the characteristics associated with the short-lived events and have important differences (Figs. 9b and c). Two general observations can be made of these long-lived events: 1) the jet core was much more elevated than the short-lived cases (between 800 hPa and 550 hPa) and 2) there was not a clear diurnal variation in LLJ intensity. The focus of these plots is on the last days of the long-lived events because that was when convection was the most widespread and it is also when we have enough soundings to cover the diurnal cycle.

For the 12 November soundings (Fig. 9b), the wind profiles were similar throughout the day, as well as the day prior (not shown). Winds above 800 hPa were continuously from the north; however, LLJs were identified for only two times during this period (2100 UTC the day prior, and 1200 UTC on 12 November; Fig. 3). In many profiles during this event, especially on 11 and 12 November, there is not a clear decrease in wind above the maximum. This lack of a distinct jet core meant many soundings did not meet the LLJ criteria. Calm to southerly wind was also present in the lower levels during this time period. At VMRS, the jet was slightly less elevated and more LLJs were identified in the soundings due to the wind speed dropping off faster with height above the jet core (not shown). Unlike 12 November, the wind profiles on 13 December (Fig. 9c) fluctuated in intensity and no discernable temporal pattern in height or intensity was found; however, distinct jet cores allowed more LLJs to be identified. The LLJ was present in separate pulses in the lower levels before being more elevated on 13 December (Fig. 8). The distinct characteristics between the short- and long-lived events imply different mechanisms might be important for jet formation and evolution.

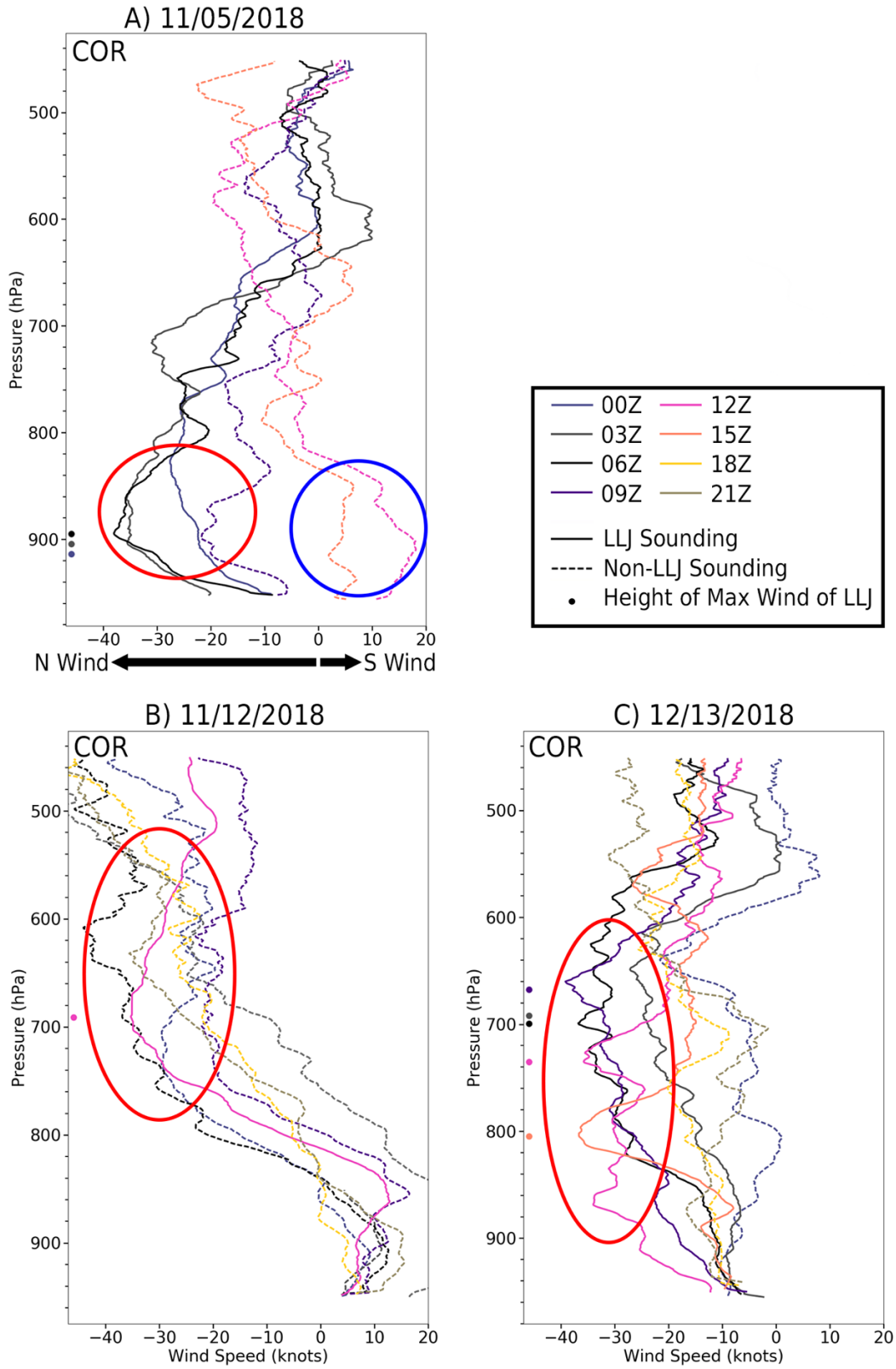

Figure 9: V-component of the wind for soundings from 24-hr periods at COR from 5 Nov (top left), 12 Nov (bottom left), and 13 Dec (bottom right). The time of the sounding is indicated by color, the dashed lines indicate soundings meeting the LLJ criteria, and the dots show the pressure level of the jet core.

To investigate boundary layer processes during the short- and long-duration LLJ events, the wind direction in the low levels (900 hPa, similar to Nicolini et al. 2004) was plotted (Fig. 10) for all 4 short-lived events and for both long-lived events. If boundary layer LLJ controls (e.g., inertial oscillation) were the dominant drivers during LLJ events, a diurnal progression of winds in the low levels would be observed. A clear rotation of low-level winds with similar timing can be seen during the short-lived events: a northeasterly wind occurred overnight (0000 to 0600 UTC), with a northwesterly wind in the morning (0600 to 1500 UTC) and a switch to the south in the afternoon (0900 to 2100 UTC). The timing and progression occurring during a single day in the short-lived cases is consistent with a role of diurnal processes such as the inertial oscillation (Blackadar 1957). The most striking difference between the short-lived cases is the timing of the switch in low-level winds to southerly. This switch occurred as early as 0900 UTC in one case and as late as 1500 UTC in another case, indicating that synoptic drivers (e.g., upper-level troughs and associated surface boundaries) may also play a role in the timing of the short-lived jets.

In contrast to the short-lived cases, no discernible diurnal progression was observed in the low-level winds during the long-lived cases. It appears that the long-lived cases are overwhelmingly, synoptically driven and the synoptic winds conceal potential diurnal cycles from boundary layer processes. Additionally, the extended large-scale forcing during these long-lived events produced widespread clouds which could have dampened diurnal cycles due to the lack of heating. Similar to the short-lived cases, a switch to southerly wind was also found near the end of the long-lived cases (Figs. 3 and 4), which is a possible indication of the progression of the upper-level pattern.

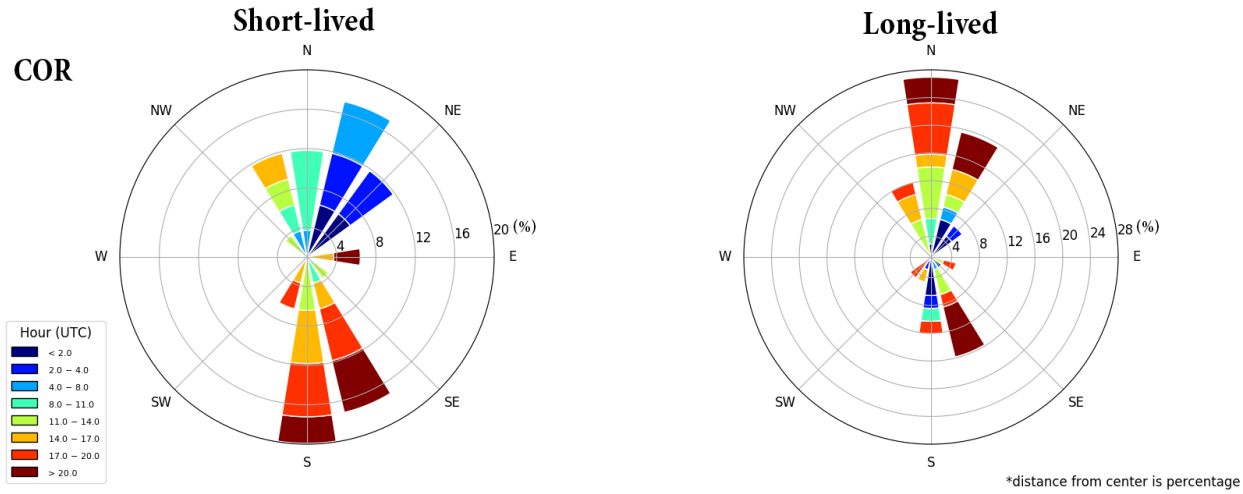

Figure 10: Diurnal cycle of winds at 900 hPa for COR for all soundings during four short-lived LLJ cases (left) and two long-lived cases (right). The short-lived LLJ cases included are: 5 November, 17 November, 22 November, 26 November. The long-lived cases are 8-12 November and 8-13 December.

3.2.2 Large-scale forcing

To fully explore the mechanisms of the SALLJ, the presence and timing of upper-level disturbances and associated low-level responses must be investigated. Synoptic maps from ERA5 (Figs. 11 and 12) show that both short- and long-lived LLJ events during RELAMPAGO coincided with a 500-hPa trough over the Pacific Ocean and an 850-hPa trough in the lee of the Andes. The SALLJ that occurred on 21-22 November is another example of a short-lived case and is similar to the 5 November short-lived case shown earlier, but the upper-level shortwave is more easily identifiable. For this reason, synoptic maps for 21-22 November are shown in Figure 11 as an example of the pattern during a short-lived LLJ event. An upper-level shortwave at 500 hPa (red circles) approached the southern Andes at 1200 UTC 21 November. As this shortwave impinged on the Andes, an 850-hPa response was observed in the form of a lee trough (orange boxes) over the sounding sites (red dots). The shortwave was south of the region where the 850-hPa lee troughing formed and where the SALLJ strengthened; therefore, it is likely that the 850-hPa high pressure to the east (blue circle) also contributed to the strengthening of the SALLJ. As the upper-level shortwave came ashore the lee troughing strengthened. Less than 24 hours after

approaching the Andes, the upper-level disturbance crossed into the Atlantic Ocean. One of the weakest shortwaves during the RELAMPAGO period was found during the 26-27 November short-lived event and occurred even farther south (not shown) leading to a weaker jet (Fig. 8). While the latitude of shortwaves and the amplitude of this pattern varied from event to event, the pattern was progressive and 850-hPa leeside troughing was present for less than 48 hours in the short-lived LLJ cases.

Synoptic maps for the 8-13 December long-lived LLJ event show many similarities to the short-lived LLJ events (Fig. 12). Upper-level disturbances passing over the Andes induced 850-hPa lee troughs, but the pattern progressed more slowly than the short-lived LLJ events. The major difference is that three 500-hPa troughs moved through in very close succession (labeled by the numbers on Fig. 12). The short gaps between these troughs meant that there was little time for the northerly flow to relax. As can be seen in the observational times series (Figs. 3 and 4) and ERA time series (Fig. 8), there were three periods of strong northerly flow, interspersed with short periods of weaker northerly flow or southerly flow. Unlike the short-lived LLJs, the southerly flow only made it as far north as COR and even this was not true for all pulses of the jet during this multi-day period (the lower dashed line in Fig. 8). This time evolution of the flow is consistent with the three troughs traversing the area one after another. The importance of the close timing of these troughs, giving little time for southerly return flow, will be discussed in the next section.

Synoptic maps for the 8-12 November long-lived LLJ episode show one very slow-moving trough during the period (Fig. 11 in Piersante et al. 2021) and the duration of northerly flow (Fig. 8) can be explained by the slow evolution of the pattern. Piersante et al. (2021) found that the 500-hPa trough over the Pacific slows and actually stalls at one point on 11 November.

The high pressure over the Pacific Ocean is shifted farther to the east than during many of the shorter LLJ events, suggesting that the high plays less of a role in the strengthening of the LLJ than the 850-hPa lee troughing. From 8-12 November, a deep layer of continuous winds from the north is present at COR and VMRS (Figs. 3 and 4), which is consistent with a slow moving, multi-day trough. Near the end of the period on 11 November, the low-level flow switched from northerly to southerly, being slightly deeper at COR than VMRS. This switch to the south was preceded by the LLJ core winds receding northward (Fig. 8). Northerly winds occurred farthest south on 8 November (mostly south of the latitudes of COR and VMRS; shown by the gray dashed lines), but by 12 November the core of the northerly low-level winds were north of COR and VMRS. This timing aligned with the position of the 850-hPa low in the lee of the Andes which drifted north through the time period (not shown) before shifting eastward (Piersante et al. 2021). During this LLJ episode, northerly flow was continuously present over a period of five days and coincident with the slow and sometimes stagnant passage of an upper-level trough.

Similar to the November long-lived case, northward movement of the lowest 850-hPa heights was also present during the short-lived LLJ cases and may contribute to the edge of northerly flow moving north and return flow from the south. Using the 21-22 November case as an example, northerly flow was present down to about 40°S at 0000 UTC on 22 November (Fig. 11). By 1200 UTC that same day, southerly flow had pushed northward and northerly flow had receded up to 30°S. Similar to the long-lived November case, the receding of the SALLJ core is visible on Figure 8 on 22 November and was present throughout all of the short-lived LLJ events. The northward movement of the lowest heights could be related to lee cyclogenesis that occurs slightly northwest of the SDC region (Fig. 11c). Accompanying frontal passages were also observed in SMN surface maps near the end of the majority of SALLJ episodes (See:

http://catalog.eol.ucar.edu/relampago). Additionally, in the short-lived cases a progressive pattern meant that the upper-level disturbances had propagated to the east of the area in 24 hours; therefore, the SDC region was on the backside of the trough where flow is from the south. Overall, we suggest from our analysis that the duration of the SALLJ events near the SDC is strongly linked with the upper-level pattern and southerly low-level flow results from the propagation of the pattern to north and then the east as discussed in Piersante et al. (2021).

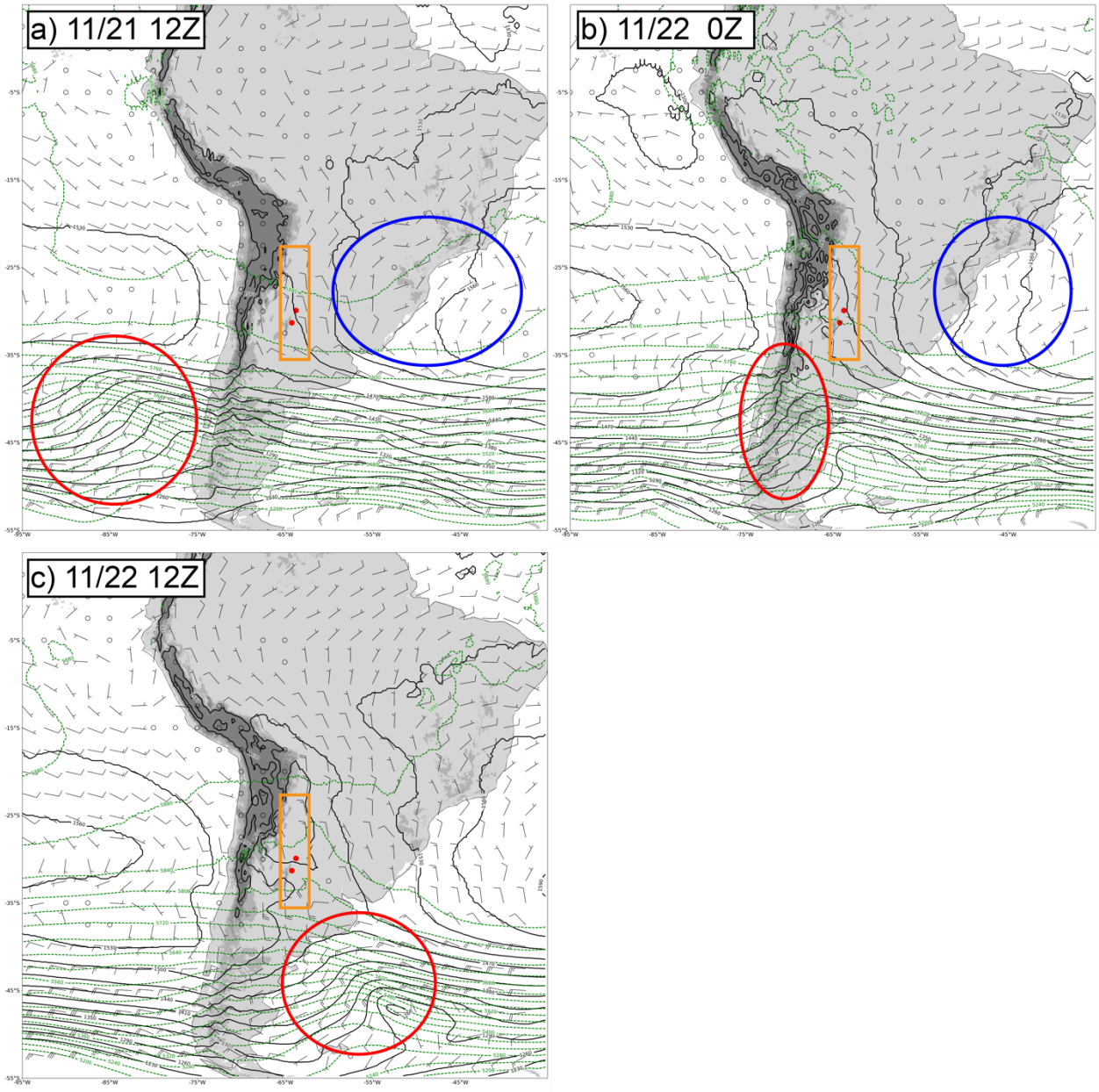

Figure 11: Twelve-hourly synoptic maps from ERA5 data for the 21-22 November case when a short-lived LLJ was observed at COR and VMRS. Terrain is shown in the shaded colors. The two red dots indicate the locations of VMRS and COR. The black solid contours and black wind barbs show 850-hPa heights and winds, respectively. The green dashed lines and green wind barbs show the same but for 500 hPa. The red circles highlight the position of the upper-level shortwave. The blue circles highlight the extension of the high pressure centered over the Atlantic Ocean. The orange boxes highlight the region in the lee the Andes where in regimes of northerly flow, the SALLJ is present near the SDC found in the bottom left of this box.

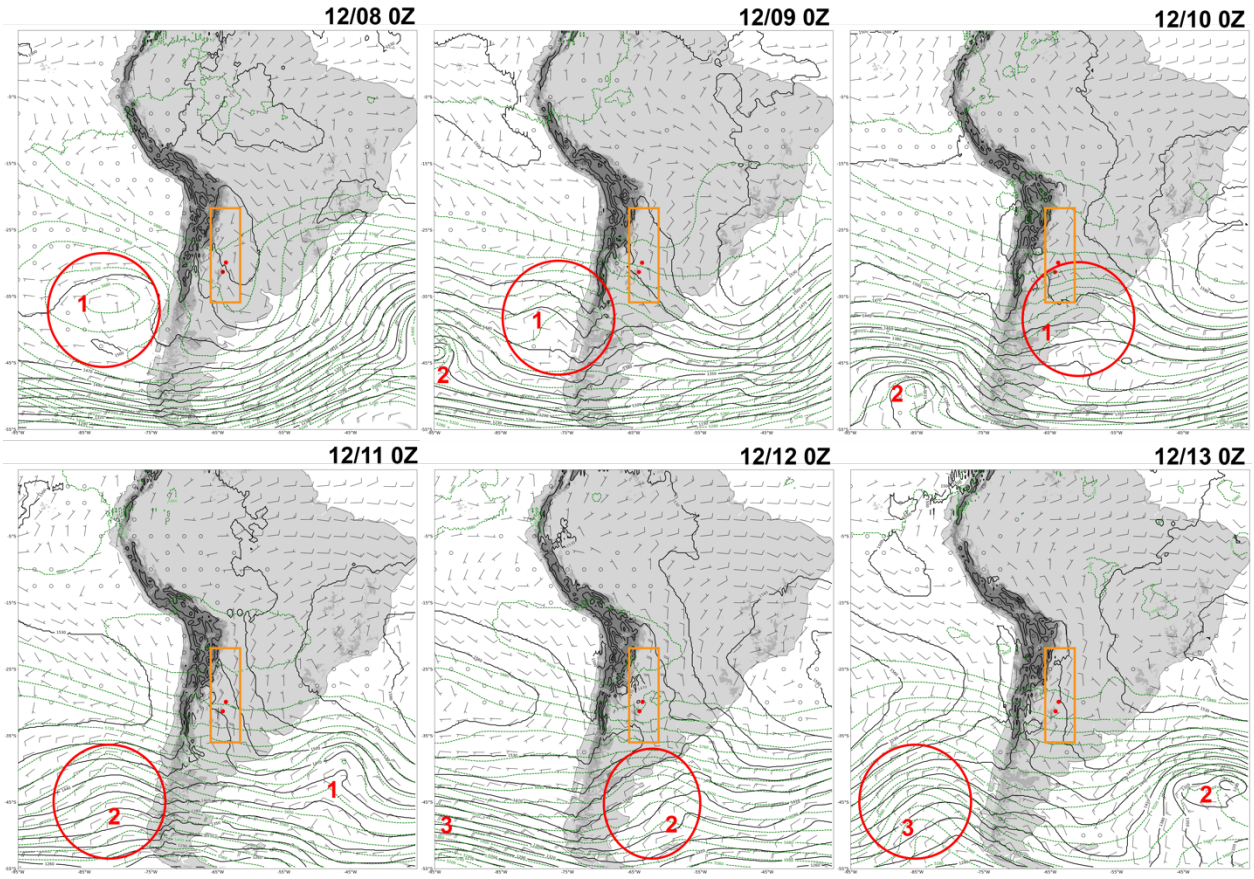

Figure 12: As in Figure 11, but daily synoptic maps for the 8-13 December case when a long-lived LLJ was observed at COR and VMRS.

To quantify the impact of synoptic forcing on the SALLJ, the east-west height difference over the area where troughing was most often present downstream of the Andes and the SALLJ occurred, is shown in Figure 13. Because of the sharpness of the lee trough (seen in map in Fig. 13), it was determined that an east-west height difference was best suited to determine the trough strength. An east-west height difference was present during all of the LLJ cases, but the strongest differences were found during the two extended LLJ cases (dark gray boxes). During the November case the height difference increased in strength as the trough slowly moved through the area. During the December case there are three clear increases in the strength of the height difference which match well with the strongest times of northerly flow from Figure 8. The 4-5 November and 26 November cases have the weakest height differences of the identified short-

lived cases (light gray shaded; Fig. 13) and also have the weakest northerly flow at COR/VMRS (Fig. 8). This relationship suggests that the strength of the 850-hPa trough is related to the strength of the LLJ and therefore connects the elevated LLJ occurrence to the passage of upper-level disturbances beyond ageostrophic circulations. Additionally, source regions of low-level air associated with the jet depend on the synoptic setup and could influence the thermodynamic impact of LLJ.

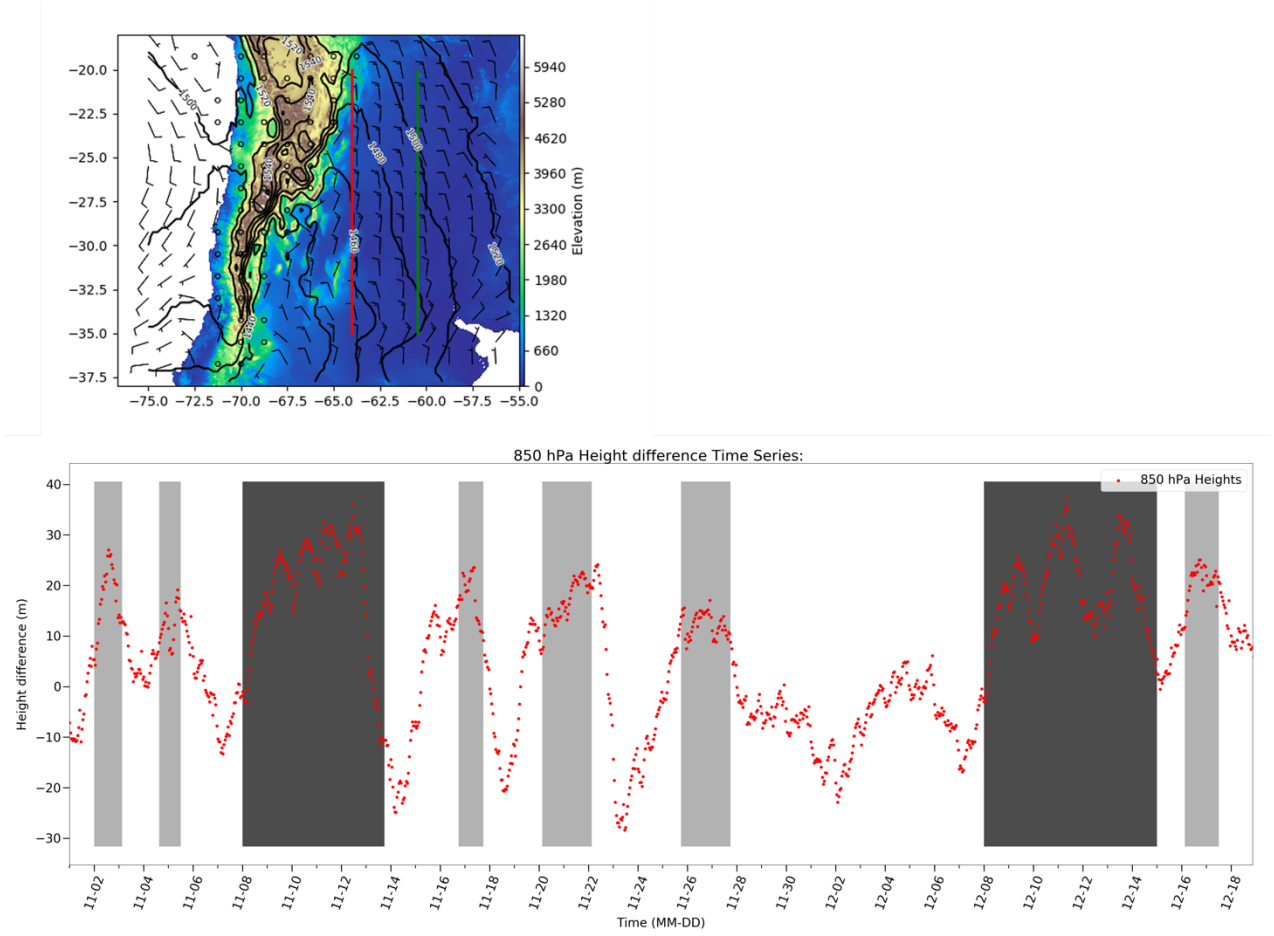

Figure 13: Time series of the east-west 850-hPa height gradient downstream of the Andes. The heights were averaged over latitudes 20-35°S and the difference was taken between 60.5 and 64°W (green line - red line). The light gray shaded areas are the short-lived LLJs and the dark gray shaded areas are the long-lived ones.

To examine the source regions and the vertical motion history of the air that arrives at VMRS and COR, the HYSPLIT model (Stein et al. 2015) was used to create 72-hour backward trajectories at the two stations. Figure 14 displays the time history of air parcels for the

observed short- and long-lived cases discussed above. Air parcels that ended at 500 hPa at VMRS and COR (green) originated from the Pacific Ocean and crossed the Andes at similar locations for all three cases (fig.14a). Trajectory pathways for air parcels ending at 700 hPa at VMRS and COR (blue) illustrate differences between the cases. For the 21 November short-lived case (black circles), the air parcel pathways traced a counter-clockwise pattern, where the air originated over northeast Argentina, curved over Paraguay and finally progressed southwards towards the SDC region. The air parcels experienced very little vertical motion and any change in height is gradual (Fig. 14b). Unlike the short-lived case, the trajectory pathways for air parcels ending at 700 hPa at VMRS and COR in the two extended LLJ cases (black squares and diamonds) were similar to the trajectory pathways for air parcels ending at 500 hPa as described above. They originated over the Pacific and crossed over the Andes. These mid-level air parcels experienced strong subsidence when they crossed the Andes, descending over 3000 ft in less than 6 hours (Fig. 14c and d). The largest differences between cases are found in the trajectories for air parcels ending at 850-hPa at VMRS and COR. In the short-lived case, the 850-hPa trajectory traced a similar counter-clockwise path as the 700 hPa trajectory, suggesting that moisture originated from the Atlantic. For the long-lived cases the low-level air originated from areas farther north and during the December case the air originated from the Amazon around 12°S. The warm, tropical temperatures of the Amazon make it a stronger moisture source than the Atlantic Ocean.

Overall, the differences between the short- and long-lived case appear in the mid- and low-level airstreams. High pressure (Fig. 11a) guides the mid-level air in the short-lived case, whereas strong subsidence over the Andes reaches into the mid levels in the long-lived cases. The differences in moisture sources are also apparent with the long-lived cases tapping into deep

tropical moisture over the Amazon while the moisture source for the short-lived cases is more likely the Atlantic Ocean.

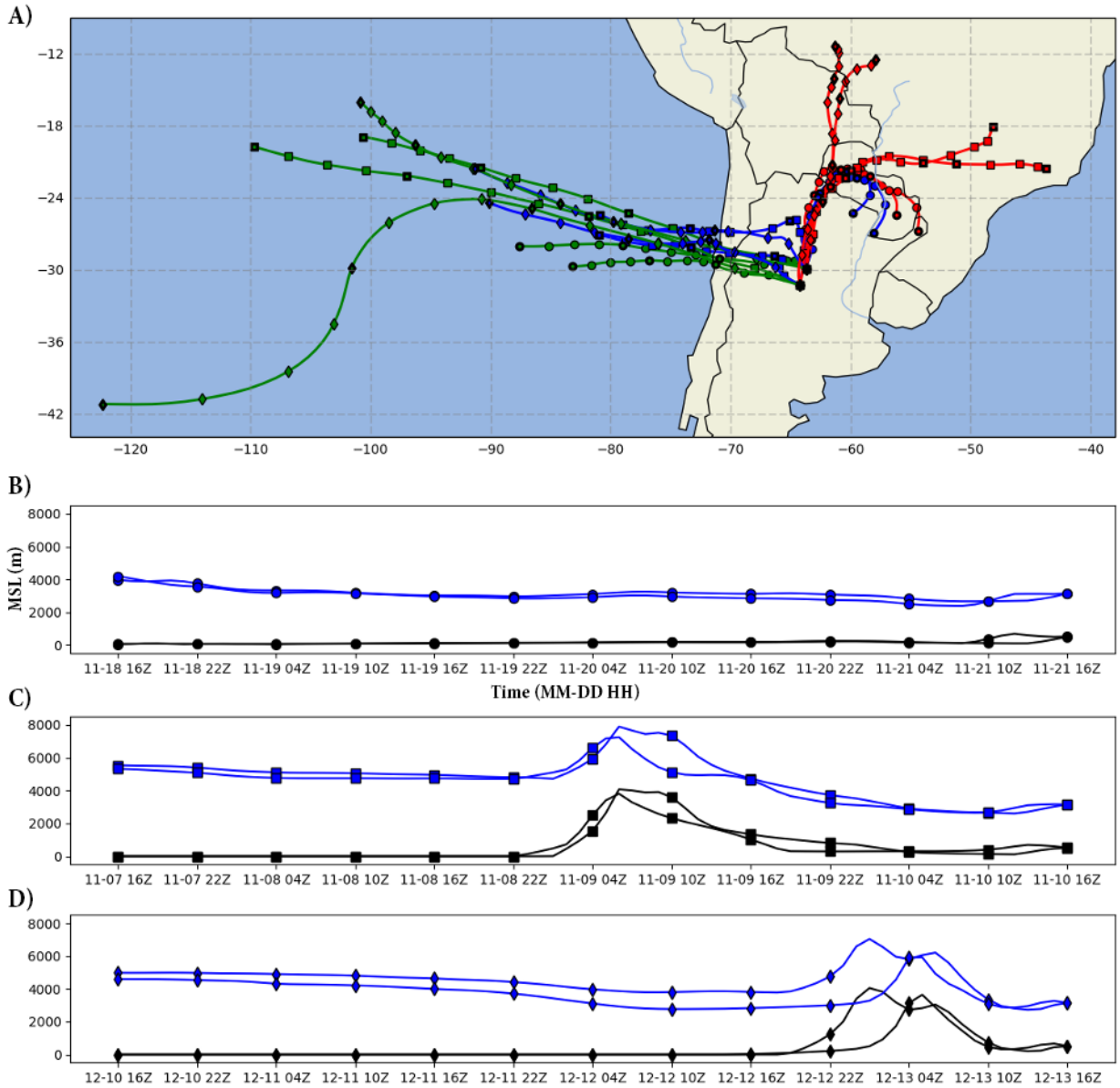

Figure 14: Seventy-two-hour backward trajectories from the HYSPLIT model ending at 1600 UTC for the three cases: 21 November, 10 November, and 13 December. The colors indicate ending height: 850-hPa (red) 700-hPa (blue), and 500-hPa (green). Points are plotted every 6 hours and the bolded points are every 24 hours. The shape of the point corresponds to each event: circle (21 November), square (10 November), and diamond (13 December). The top map shows the horizontal tracks with the bottom plots showing the vertical movement of air through time for 700-hPa. The black lines on the bottom plots show the terrain height along the trajectory.

3.3 SALLJ impacts on moisture availability and the presence of convection

The influence of the different 850-hPa air streams is evident from a N-S Hovmöller of 850-hPa specific humidity produced using ERA5 data (Fig. 15). The v-winds greater than 20 kts are overlaid with northerly/southerly winds represented by dashed/solid lines. Moisture levels were higher (>10 g/kg) at the latitudes of VMRS and COR (gray dashed lines) around the times of strong northerly flow (dashed lines). During the two long-lived LLJ events in the black boxes, increased moisture was present for extended periods (> 3 days). Throughout these events specific humidity was higher (13-16 g/kg) than many of the short-lived cases. This observation is particularly apparent near the end of these periods when the highest moisture values occurred. Furthermore, moisture extended farther south with >10 g/kg reaching 35°S and was deeper at 35°S during the long-lived cases than in the short-lived cases. These time periods coincided with long-duration northerly flow and where the 850-hPa flow was traced to areas farther north (Fig. 14). The higher amounts of moisture are consistent with the strong connection to the Amazon as the moisture source. The short-lived case on 16-17 December is an exception to the pattern of moisture being more limited south of the SDC region during the short-lived cases; however, this case follows the December long-lived event which could be seen as pre-moistening the area.

Convective coverage was calculated as the area downstream of the SDC with GOES-16 IR temperatures less than 235K (Fig. 16). Northerly LLJ periods are shaded with short-lived events in light gray and long-lived in dark gray. These LLJ periods that had increased moisture (>10 g/kg, Fig. 15), were also concurrent with periods of extensive convection downstream of the SDC (Fig. 16). Within each event, convective coverage tended to peak near the end or just after the period of strongest northerly flow. This timing could be the result of a combination of impacts of the SALLJ including continued moisture transport, thermodynamic destabilization,

vertical wind shear, and low-level convergence. The highest convective coverage occurred during the two extended LLJ events when about half to three quarters of the area was covered. Convection was also widespread during the short-lived LLJ event on 17 December. The highest levels of moisture were found at these times (Fig. 15), but additional factors discussed above might also be increased due to the longevity of the LLJ. Moisture is only one ingredient necessary for convection and the connection between the SALLJ and the convective environment must be further investigated through RELAMPAGO observations.

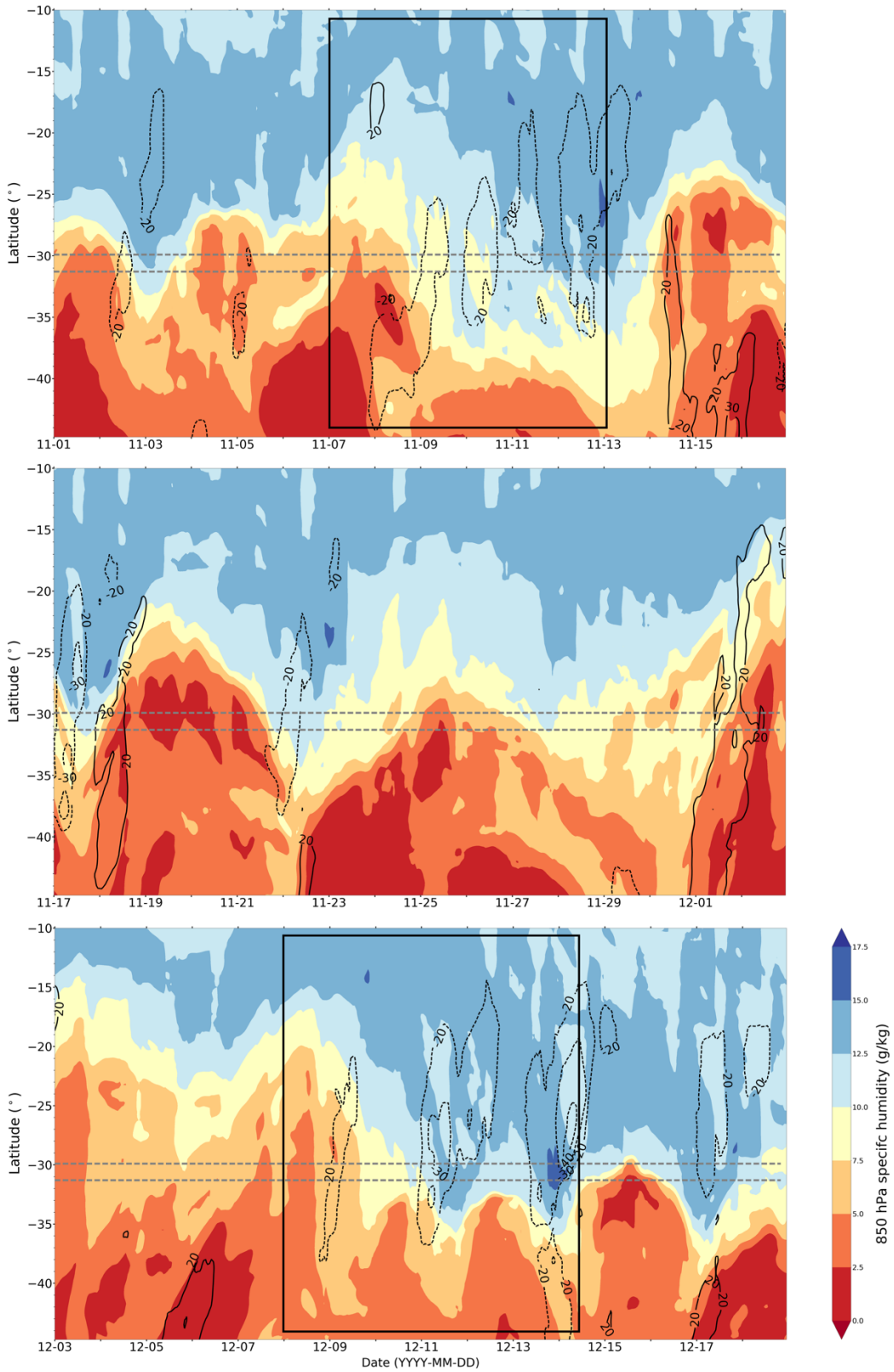

Figure 15: N-S Hovmöller diagram of 850-hPa specific humidity (shaded) and v-wind > 20 kts (dashed contours from north, solid from south) averaged over -55° to -65° W using ECMWF Reanalysis 5 (ERA5). Dash-dot lines show the latitude of VMRS (upper) and COR (lower). The black boxes are the two extended northerly LLJ events from the observational plots.

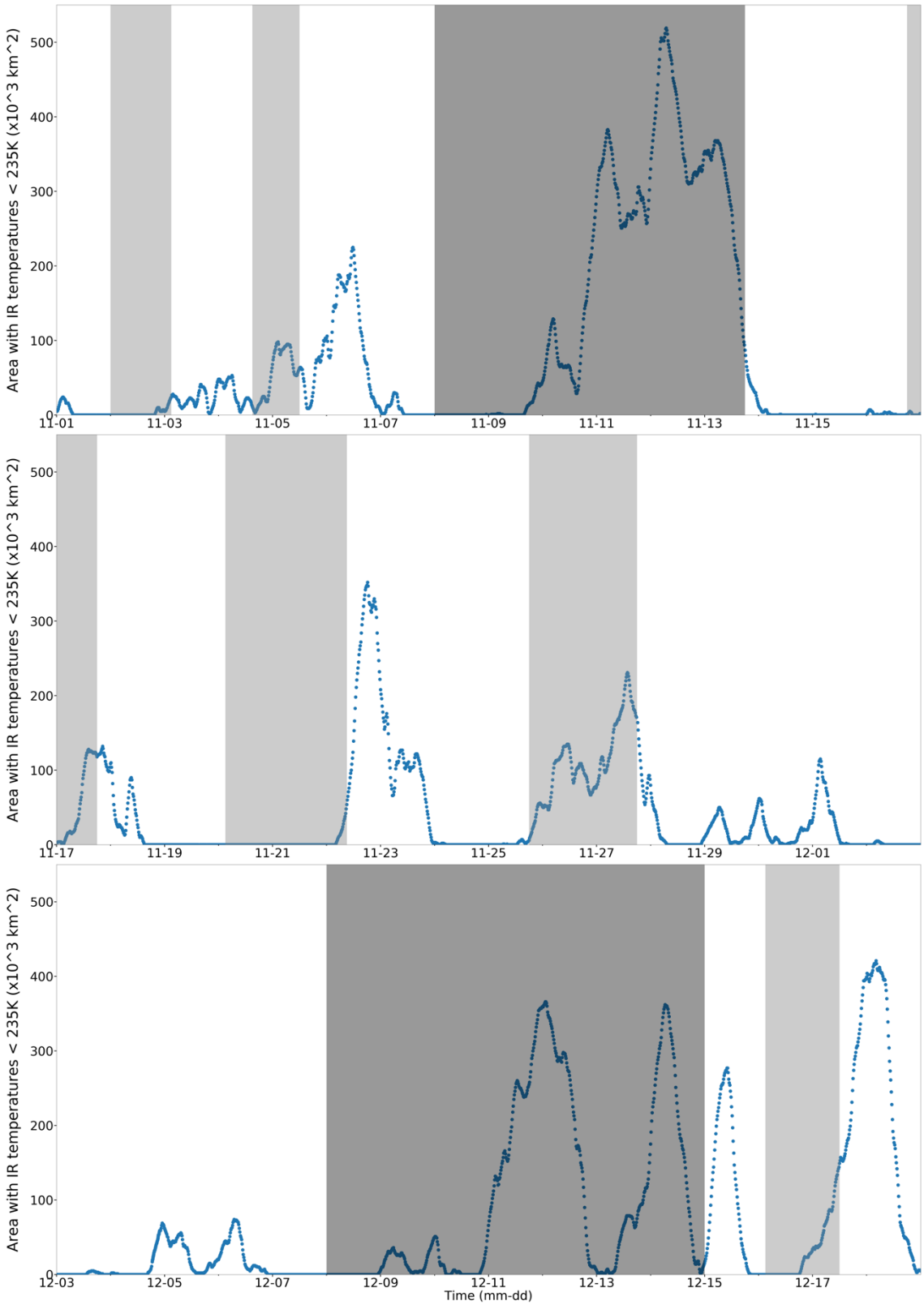

Figure 16: Time series of area with GOES-16 IR temperatures less than 235 K. The region used (29-35°S and 55-65°W) was an area downstream of the SDC (black box Fig. 1). The total area of the region is 726,000 km^2. The gray circles represent the shorter northerly LLJ events identified in the Figure 8 above with the black being the longer-duration LLJ events.

Chapter 4.
DISCUSSION

Our findings are broadly consistent with past studies of the SALLJ. The short-lived events observed during RELAMPAGO share characteristics with NLLJs such as an overnight peak and counter-clockwise wind gyre and with previous analyses of the SALLJ using SALLJEX observations (Vera et al. 2006; Nicolini et al. 2004), reanalysis data (e.g., Marengo et al. 2004), and model output (e.g., Nicolini and Saulo 2006). Similar to Salio et al. (2002), these short-lived events were observed most frequently and therefore represent the mean SALLJ; however, the observations shown in Figure 6 verified that the height of jet cores varied quite widely and could be more elevated, up to 650 hPa, such as noted in ONK18. Near the end of the two long-lived LLJ events, the jet was found higher in the atmosphere and its intensity did not appear to follow a diurnal cycle. The characteristics of this jet aligned more closely with a LLJS than a NLLJ. The distinct characteristics of the jets during these long-lived events motivated a closer look at the mechanisms driving the SALLJ and their impact on SALLJ characteristics.

Our analysis revealed the presence of synoptic forcing in all RELAMPAGO SALLJ cases, evidenced by upper-level troughs traversing the Andes followed by the presence of lee cyclogenesis and subsidence during both short- and long-lived SALLJ events. Nicolini et al. (2004b) hypothesized a large-scale pattern involving a low in Northwestern Argentina in the lee of the Andes that works with the Atlantic High to extend the SALLJ down into Argentina. Modeling work of a case study by Rasmussen and Houze (2016) further found that the extreme height of the Andes controlled the strength of lee cyclogenesis and the SALLJ. Our finding that the greatest east-west height differences at 850 hPa and 700 hPa occurred during identified

SALLJ periods along with upper-level disturbances is consistent with lee cyclogenesis playing an important role in SALLJ episodes (Fig. 13). Expanding upon the large-scale influence proposed in Nicolini et al. (2004b), this study found that lee troughing played a more dominant role than the Atlantic High during the long-lived LLJ events, particularly during the 8-12 November event. This result could be explained by the unseasonably strong upper-level trough identified by Piersante et al. (2021). During the short-lived cases, high pressure acted to strengthen the low-level gradient, especially when the upper-level trough (and corresponding lee troughing) was weaker than in the long-lived cases or located farther south of the RELAMPAGO domain.

Furthermore, the duration of SALLJ events is tied to the upper-level pattern. Progressive patterns with spaced out troughs coincided with short-lived SALLJs while closely spaced or quasi-stationary troughs coincided with long-lived SALLJ episodes. Different upper-level patterns were observed during each of the two long-lived LLJ events. During the 8-12 November case, a quasi-stationary trough was present (Piersante et al. 2021) leading to continuous northerly flow whereas during 8-13 December, the pattern was more progressive with three upper-level troughs moving through the area in close succession producing three pulses of northerly flow. The closeness of the troughs during the December long-lived event meant that an 850-hPa height difference persisted for multiple days and southerly flow did not reach the SDC region (Fig. 8).

Prior work hypothesized an association of synoptic forcing with specific SALLJ characteristics, but these relationships were not well documented. This RELAMPAGO analysis was able to tie periods of extended synoptic activity and their unique setup to long-lived and elevated SALLJ cases, confirming hypotheses from Saulo et al. 2004 and ONK18. Building on the relationship between subsidence and the strengthening of the lee low established by Seluchi

et al. (2003), this study found that deep layers of subsidence were present during long-lived events (Fig. 14c and d). This pattern likely contributed to the strong 850-hPa gradients (Fig. 13) observed during periods of deeper LLJs.

The SALLJ can also be tied to moisture transport and convection. In particular, the longer duration SALLJ events greatly increased the environmental moisture deep into Central Argentina. Prior reanalysis studies (e.g., Nogues-Paegle and Mo 1997) have shown that the SALLJ transports moisture south from the Amazon to the midlatitudes. Our findings confirm that the Amazon is the moisture source during our two long-lived cases (Fig. 12); however, low-level air appears to be transported in from the colder Atlantic Ocean in the short-lived cases (Fig. 11), suggesting a different moisture source. The moisture in the short-lived cases being fed by a weaker source aligns with the slightly lower amounts of moisture observed in reanalysis data that may influence the impact of the SALLJ on convection (e.g., Saulo et al. 2007; Salio et al 2007; Borque et al. 2010).

Chapter 5.
CONCLUSIONS

This study was able to build on prior research by explaining a typology of the SALLJ based on observations, providing more evidence of its drivers, and inferring initial links to widespread convection near the SDC. Using high temporal soundings obtained during RELAMPAGO along with ERA5 data, we examined the variability and characteristics of the SALLJ in Central Argentina and found the presence of nocturnal LLJs and elevated LLJs with no clear discernable diurnal cycle that were characterized as short-lived and long-lived northerly LLJ events, respectively. Our primary results are summarized as follows:

- The short-lived SALLJ events found in this study are similar to the mean SALLJ signature highlighted in previous studies across South America. These short-lived events were the most frequent SALLJ periods during RELAMPAGO and had characteristics resembling those of a NLLJ, including peaking overnight at or below 850 hPa. Evidence of both boundary layer processes driven by diurnal heating and synoptic-scale features, including progressive upper-level troughs with associated lee cyclogenesis near the SDC, were found during these short-lived events.
- Two longer-duration SALLJ events were observed during RELAMPAGO with the LLJ being more elevated (i.e., peaking above 850 hPa) near the end of these periods. These long-lived SALLJ events had characteristics resembling those of a LLJS, and synoptic drivers appeared to be dominant. In particular, quasi-stationary troughs or upper-level troughs moving through the area in close succession produced extended periods of lee cyclogenesis with stronger east-west pressure gradients than during short-lived periods.
- Trajectory analyses suggest that direct moisture transport from the Amazon may be a unique feature of the long-lived SALLJ events, greatly increasing the environmental

moisture deep into Central Argentina, especially near the SDC. In the short-lived cases, moisture appeared to originate over the colder Atlantic Ocean and therefore slightly lower amounts were present.

- While moisture is only one ingredient in determining convective potential, the most widespread convection occurred near the end or just after SALLJ periods, with greatest coverage at the end of long-lived events when the jet was most elevated and high levels of moisture were present.

These findings will enable future research to understand the points in the convective lifecycle in which the SALLJ has an influential role. This study was able to identify specific characteristics of long-lived LLJ events during times of widespread convection which allows us to begin to test theories of synergism between the jet and convection such as those in Saulo et al. (2007). One hypothesis is that the jet has a role in maintaining and organizing convection through continued moisture transport, enhanced low-level convergence, and the presence of strong vertical shear. Near the end of the long-lived events, the jet is elevated and features southerly undercutting flow, creating strong wind shear which we believe may aid in the rapid organization of convection (e.g., Piersante et al. 2021). With high-resolution observations and reanalysis available from the RELAMPAGO period, along with high-resolution model simulations during these convection events, future research will more closely examine the relationship of environmental characteristics produced by the jet (e.g., wind shear and low-level convergence), the terrain (ex. subsidence), and the upper-level jet stream (ex. upper-level divergence) with respect to the convective lifecycle, including the relationship between the SDC, SALLJ flow patterns, and rapid upscale growth of convection.

BIBLIOGRAPHY

Anabor, V., D. J. Stensrud, and O. L. L. De Moraes, 2008: Serial upstream-propagating mesoscale convective system events over southeastern South America. *Mon. Weather Rev.*, **136**, 3087–3105, https://doi.org/10.1175/2007MWR2334.1.

Blackadar, A. K., 1957: Boundary Layer Wind Maxima and Their Significance for the Growth of Nocturnal Inversions. *Bull. Am. Meteorol. Soc.*, **38**, 283–290, https://doi.org/10.1175/1520-0477-38.5.283.

Bonner, W. D., 1968: Climatology of the Low Level Jet. *Mon. Weather Rev.*, **96**, 833–850, https://doi.org/10.1175/1520-0493(1968)096<0833:cotllj>2.0.co;2.

Borque, P., P. Salio, M. Nicolini, and Y. G. Skabar, 2010: Environment associated with deep moist convection under SALLJ conditions: A case study. *Weather Forecast.*, **25**, 970–984, https://doi.org/10.1175/2010WAF2222352.1.

Byerle, L. a, and J. Paegle, 2002: Description of the seasonal cycle of low-level flows flanking the Andes and their interannual variability. *Meteorologica*, **27**, 71–88.

Campetella, C. M., and C. S. Vera, 2002: The influence of the Andes mountains on the South American low-level flow. *Geophys. Res. Lett.*, **29**, 6–9, https://doi.org/10.1029/2002GL015451.

Carril, A. F., and Coauthors, 2012: Performance of a multi-RCM ensemble for South Eastern South America. *Clim. Dyn.*, **39**, 2747–2768, https://doi.org/10.1007/s00382-012-1573-z.

Carvalho, L. M. V., and C. Jones, 2001: A satellite method to identify structural properties of mesoscale convective systems based on the maximum spatial correlation tracking technique (MASCOTTE). *J. Appl. Meteorol.*, **40**, 1683–1701, https://doi.org/10.1175/1520-0450(2001)040<1683:ASMTIS>2.0.CO;2.

Chen, Y.-L., X. A. Chen, and Y.-X. Zhang, 1994: A Diagnostic Study of the Low-Level Jet during TAMEX IOP 5. *Mon. Weather Rev.*, **122**, 2257–2284.

Du, Y., Q. Zhang, Y. L. Chen, Y. Zhao, and X. Wang, 2014: Numerical simulations of spatial distributions and diurnal variations of low-level jets in China during early summer. *J. Clim.*, **27**, 5747–5767, https://doi.org/10.1175/JCLI-D-13-00571.1.

Du, Y., Q. Zhang, Y. Ying, and Y. Yang, 2012: Characteristics of low-level jets in Shanghai during the 2008-2009 warm seasons as Inferred from wind profiler radar data. *J. Meteorol. Soc. Japan*, **90**, 891–903, https://doi.org/10.2151/jmsj.2012-603.

Hersbach, H., and Coauthors, 2020: The ERA5 global reanalysis. *Q. J. R. Meteorol. Soc.*, **146**, 1999–2049, https://doi.org/10.1002/qj.3803.

Hoecker, W., 1963: Three southerly low-level jet systems de- lineated by the weather Bureau Special Pibal Network of 1961. *Mon. Weather Rev.*, **91**, 573–582.

Holton, J. R., 1967: The diurnal boundary layer wind oscillation above sloping terrain. *Tellus*, **19**, 200–205, https://doi.org/10.3402/tellusa.v19i2.9766.

Houze, R. A., K. L. Rasmussen, M. D. Zuluaga, and S. R. Brodzik, 2015: The variable nature of convection in the tropics and subtropics: A legacy of 16 years of the Tropical Rainfall Measuring Mission satellite. *Rev. Geophys.*, **53**, 994–1021, https://doi.org/10.1002/2015RG000488.

Liu, C., and E. J. Zipser, 2015: The global distribution of largest, deepest, and most intense precipitation systems. *Geophys. Res. Lett.*, **42**, 3591–3595, https://doi.org/10.1002/2015GL063776.

Marengo, J. A., W. R. Soares, C. Saulo, and M. Nicolini, 2004: Climatology of the low-level jet east of the Andes as derived from the NCEP-NCAR reanalyses: Characteristics and temporal variability. *J. Clim.*, **17**, 2261–2280, https://doi.org/10.1175/1520-0442(2004)017<2261:COTLJE>2.0.CO;2.

Montini, T. L., C. Jones, and L. M. V. Carvalho, 2019: The South American Low-Level Jet: A New Climatology, Variability, and Changes. *J. Geophys. Res. Atmos.*, **124**, 1200–1218, https://doi.org/10.1029/2018JD029634.

Mulholland, J. P., S. W. Nesbitt, R. J. Trapp, K. L. Rasmussen, and P. V. Salio, 2018: Convective storm life cycle and environments near the Sierras de Córdoba, Argentina. *Mon. Weather Rev.*, **146**, 2541–2557, https://doi.org/10.1175/MWR-D-18-0081.1.

Nascimento, M. G., D. L. Herdies, and D. O. De Souza, 2016: The south American water balance: The influence of low-level jets. *J. Clim.*, **29**, 1429–1449, https://doi.org/10.1175/JCLI-D-15-0065.1.

Nesbitt, S. W., R. Cifelli, and S. A. Rutledge, 2006: Storm morphology and rainfall characteristics of TRMM precipitation features. *Mon. Weather Rev.*, **134**, 2702–2721, https://doi.org/10.1175/MWR3200.1.

Nesbitt, S. W., and coauthors, 2021: A storm safari in Argentina, Proyecto RELAMPAGO. *Bull. Amer. Meteor. Soc.*, conditionally accepted.

Nicolini, M. and A. C. Saulo, 2000: Eta characterization of the 1997-1998 warm season Chaco jet cases. Preprints 6th International Conference on Southern Hemisphere Meteorology and Oceanography, Chile, 330-331.

Nicolini, M., and A. C. Saulo, 2006: Modeled Chaco low-level jets and related precipitation patterns during the 1997-1998 warm season. *Meteorol. Atmos. Phys.*, **94**, 129–143, https://doi.org/10.1007/s00703-006-0186-7.

Nicolini, M., A. C. Saulo, J. C. Torres, and P. Salio, 2002: Enhanced Precipitation Over Southeastern South America Related To Strong Low-Level Jet Events During Austral Warm Season. *Meteorol. Spec. Issue South Am. Monsoon Syst.*, **27**, 59–69.

Nicolini, M., P. Salio, G. Ulke, J. Marengo, M. Douglas, J. Paegle, and E. Zipser, 2004: South American Low-level jet diurnal cycle and three dimensional structure. *CLIVAR Exch.*, **9**, 6–8.

Nicolini, M., P. Salio and J. Paegle, 2004b: Diurnal wind cycle of the South American Low-Level Jet. 1st International CLIVAR Science Conference. Poster session 2: Monsoon Systems, June 21-25, 2004, Baltimore, Maryland, USA. MS-80.

Nogués-Paegle, J., and K. C. Mo, 1997: Alternating wet and dry conditions over South America during summer. *Mon. Weather Rev.*, **125**, 279–291, https://doi.org/10.1175/1520-0493(1997)125<0279:AWADCO>2.0.CO;2.

Oliveira, M. I., E. L. Nascimento, and C. Kannenberg, 2018: A new look at the identification of low-level jets in South America. *Mon. Weather Rev.*, **146**, 2315–2334, https://doi.org/10.1175/MWR-D-17-0237.1.

Paegle, J., 1998: A comparative review of South American low level jets. Meteorologica, **23**, 73–81.

Piersante, J. O., K. L. Rasmussen, R. S. Schumacher, A. K. Rowe, and L. A. McMurdie, 2021: A Synoptic Evolution Comparison of the Largest MCSs in Subtropical South America between Spring and Summer. *Mon. Weather Rev.,* conditionally accepted.

Rasmussen, K. L., M. D. Zuluaga, and R. A. Houze, 2014: Severe convection and lightning in subtropical South America. *Geophys. Res. Lett.*, **41**, 7359–7366, https://doi.org/10.1002/2014GL061767.

Rasmussen, K. L., M. M. Chaplin, M. D. Zuluaga, and R. A. Houze, 2016: Contribution of extreme convective storms to rainfall in South America. *J. Hydrometeorol.*, **17**, 353–367, https://doi.org/10.1175/JHM-D-15-0067.1.

Rasmussen, K. L., and R. A. Houze, 2016: Convective initiation near the Andes in subtropical South America. *Mon. Wea. Rev.*, **144**, 2351–2374, https://doi.org/10.1175/MWR-D-15-0058.1.

Rasmusson, E. M., and K. C. Mo, 1996: Large-Scale Atmospheric Moisture Cycling As Evaluated from NMC Global Analysis and Forecast Products. *J. Clim.*, **9**, 3276–3297.

Repinaldo, H. F. B., M. Nicolini, and Y. G. Skabar, 2015: Characterizing the diurnal cycle of low-level circulation and convergence using CFSR data in southeastern South America. *J. Appl. Meteorol. Climatol.*, **54**, 671–690, https://doi.org/10.1175/JAMC-D-14-0114.1.

Rife, D. L., J. O. Pinto, A. J. Monaghan, C. A. Davis, and J. R. Hannan, 2010: Global distribution and characteristics of diurnally varying low-level jets. *J. Clim.*, **23**, 5041–5064, https://doi.org/10.1175/2010JCLI3514.1.

Salio, P., M. Nicolini, and A. C. Saulo, 2002: Chaco low-level jet events characterization during the austral summer season. *J. Geophys. Res. Atmos.*, **107**.

Salio, P., M. Nicolini, and E. J. Zipser, 2007: Mesoscale convective systems over southeastern South America and their relationship with the South American low-level jet. *Mon. Weather Rev.*, **135**, 1290–1309, https://doi.org/10.1175/MWR3305.1.

Saulo, A. C., M. E. Seluchi, and M. Nicolini, 2004: A Case Study of a Chaco Low-Level Jet Event. *Mon. Weather Rev.*, **132**, 2669–2683, https://doi.org/10.1175/MWR2815.1.

Saulo, C., J. Ruiz, and Y. G. Skabar, 2007: Synergism between the low-level jet and organized convection at its exit region. *Mon. Weather Rev.*, **135**.

Seluchi, M. E., A. C. Saulo, M. Nicolini, and P. Satyamurty, 2003: The Northwestern Argentinean Low: A study of two typical events. *Mon. Weather Rev.*, **131**, 2361–2378, https://doi.org/10.1175/1520-0493(2003)131<2361:TNALAS>2.0.CO;2.

Servicio Meteorológico Nacional-Argentina, 2019: SMN Radiosonde Data. Version 1.0. https://doi.org/10.26023/E8MP-0GD3-4903.

Shapiro, A., E. Fedorovich, and S. Rahimi, 2016: A unified theory for the great plains nocturnal low-level jet. *J. Atmos. Sci.*, **73**, 3037–3057, https://doi.org/10.1175/JAS-D-15-0307.1.

Silvers, L. G., and W. H. Schubert, 2012: A theory of topographically bound balanced motions and application to atmospheric low-level jets. *J. Atmos. Sci.*, **69**, 2878–2891, https://doi.org/10.1175/JAS-D-11-0309.1.

Stein, A. F., R. R. Draxler, G. D. Rolph, B. J. B. Stunder, M. D. Cohen, and F. Ngan, 2015: Noaa's hysplit atmospheric transport and dispersion modeling system. *Bull. Am. Meteorol. Soc.*, **96**, 2059–2077, https://doi.org/10.1175/BAMS-D-14-00110.1.

Stensrud, D. J., 1996: Importance of Low-Level Jets to Climate: A Review. *J. Clim.*, **9**, 1698–1710.

UCAR/NCAR-Earth Observing Laboratory, 2020: Multi-Network Composite Highest Resolution Radiosonde Data. Version 1.3. https://doi.org/10.26023/GKFF-YNBJ-BV14.

Uccellini, L. W., 1980: On the Role of Upper Tropospheric Jet Streaks and Leeside Cyclogenesis in the Development of Low-Level Jets in the Great Plains. *Mon. Weather Rev.*, **108**, 1689–1696.

Vera, C., and Coauthors, 2006: The South American Low-Level Jet Experiment. *Bull. Am. Meteorol. Soc.*, **87**, 63–78.

Vila, D. A., L. A. T. Machado, H. Laurent, and I. Velasco, 2008: Forecast and tracking the evolution of cloud clusters (ForTraCC) using satellite infrared imagery: Methodology and validation. *Weather Forecast.*, **23**, 233–245, https://doi.org/10.1175/2007WAF2006121.1.

Zipser, E. J., D. J. Cecil, C. Liu, S. W. Nesbitt, and D. P. Yorty, 2006: Where are the most: Intense thunderstorms on Earth? *Bull. Am. Meteorol. Soc.*, **87**, 1057–1071, https://doi.org/10.1175/BAMS-87-8-1057.

Appendix A.
ERA5 EVALUATION

While RELAMPAGO produced high temporal ground-based observations in Central Argentina, the observations were still limited in time and particularly in space. The observations provided 3-hourly soundings during IOPs allowing for the identification of SALLJ episodes of varying duration. However, with the reduction of soundings outside of these IOPs, it is difficult to clearly determine the start and stop times of these enhanced northerly flow events. The hourly ERA5 dataset allows for us to fill in these temporal gaps. Further, station-based observational data is too limited for synoptic-scale analysis; therefore, ERA5 is necessary to understand the influence of the synoptic environment on the presence and evolution of the SALLJ.

In order to use ERA5 to analyze synoptic-scale flow and moisture patterns, ERA5 winds and moisture were evaluated against the COR and VMRS sounding data (Figs. A1 and A2). With respect to winds, the data from ERA5 overall compared well to the observations. The magnitude of the errors was slightly smaller for the more elevated winds (850-700 hPa) than the lower levels (950-850 hPa). The largest errors are found at COR in the lower levels along with a consistent low bias that is similar in magnitude. Thus, the errors in magnitude are likely explained by the low bias. Errors in the low levels at COR could be due to the representation of the topography in the ERA model and small discrepancies could partially be explained by balloon drift. Overall, for our purposes in identifying periods of increased northerly flow over Central Argentina, ERA5 captures the general flow pattern present in the observations and can be used to extend our analysis in time and space. Additionally, moisture is transported by LLJs and is a necessary component of convection; therefore, it is important that the ERA5 correctly represents moisture for our efforts in evaluating the extent and magnitude of moisture transport

from the north. The ERA5 does well in representing full column precipitable water (PW). At both stations the average error is less than 4 mm. At COR the PW is consistently slightly overestimated, but the bias is less consistent at VMRS. Again, the column PW from ERA5 compares very well to the PW from the observed soundings.

The 850-hPa-700-hPa wind shear was calculated and compared as it is important in identifying the most common LLJs. Overall, ERA5 is able to capture the correct sign of wind shear, but with large errors in the magnitude that hinders the ability of ERA5 to capture LLJs using our objective identification method. ERA5 had the correct sign for 84% and 74% of the soundings at COR and VMRS, respectively, but the average magnitudinal error was found to be 5-7 kts. It is important to note that, in calculating fixed-level shear, small spatial and temporal errors can exacerbate magnitudinal errors. These temporal errors may also contribute to diminished LLJ frequency in ERA5 data. In this case, about half of the LLJs found in the observed soundings were identified as LLJs in ERA5 (not shown). Prior research has documented similar challenges in capturing LLJs in reanalysis (e.g., Walters et al. 2014). Broadly, wind shear is not only important in the identification of LLJs but in convective organization overall. For these reasons, ERA5 data is not used for a detailed analysis of the SALLJ through objective identification in our study, but it is acceptable for describing the evolution of synoptic-scale wind patterns and moisture transport.

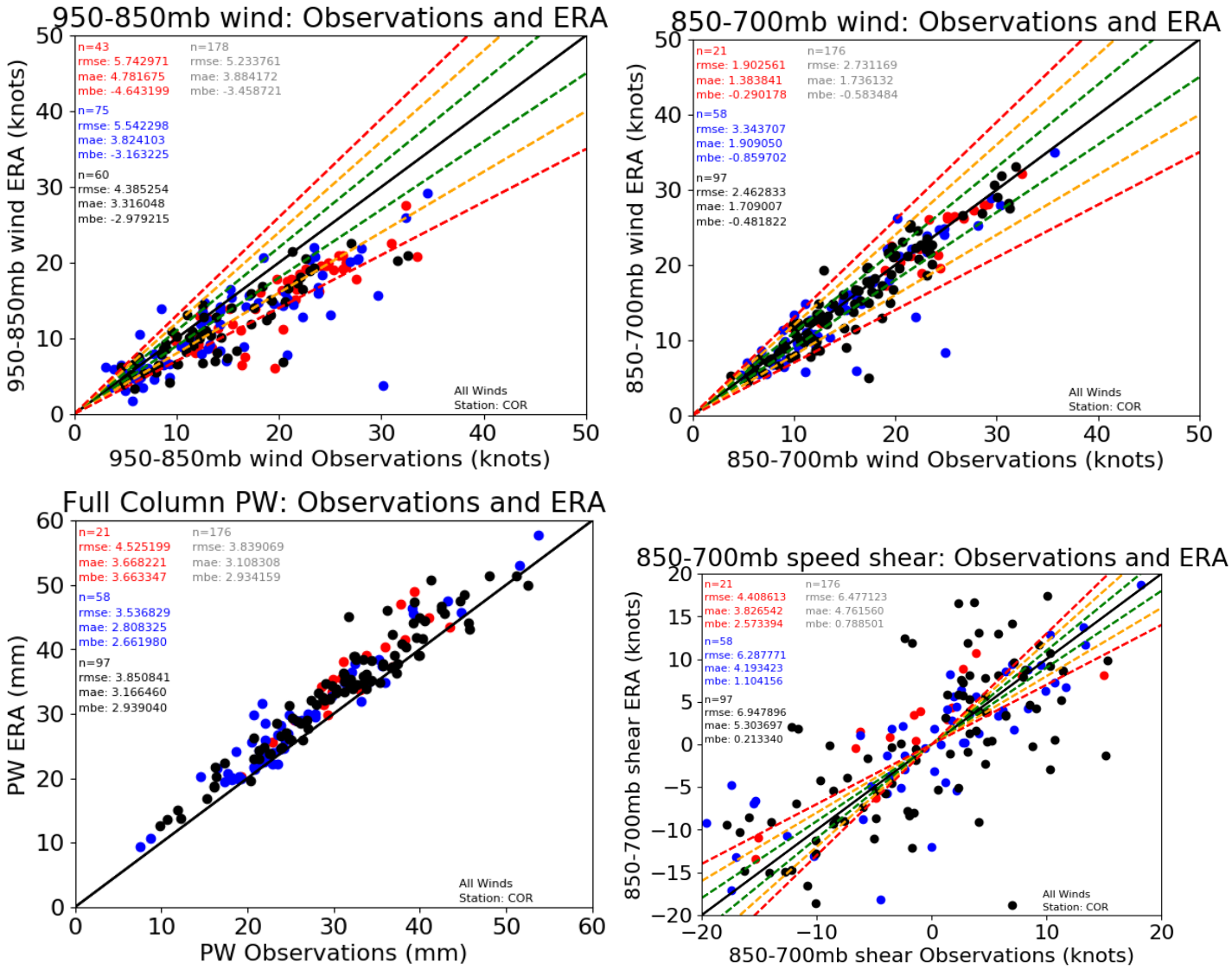

Figure A1: Comparison of wind speeds and moisture in the ERA5 and observational soundings for COR. The value found in the ERA5 dataset is on the y-axis and the value observed from soundings is on the x-axis for winds in the 950-850-hPa layer (top left), winds in the 850-700-hPa layer (top right), full column precipitable water (bottom left), and 850-700-hPa speed shear (bottom right). Color indicates the most common wind direction in the area of interest with red from the north, blue from the south, and black from the east or west. The black solid line indicates the same value in ERA5 as in observations. The green, orange, and red dashed lines are 10, 20 and 30% error respectively. The numbers in the top left are statistics: number of samples, root mean squared error (RMSE), mean absolute error (MAE), and mean bias error (MBE). All the plots compare values at all times when observations were taken.

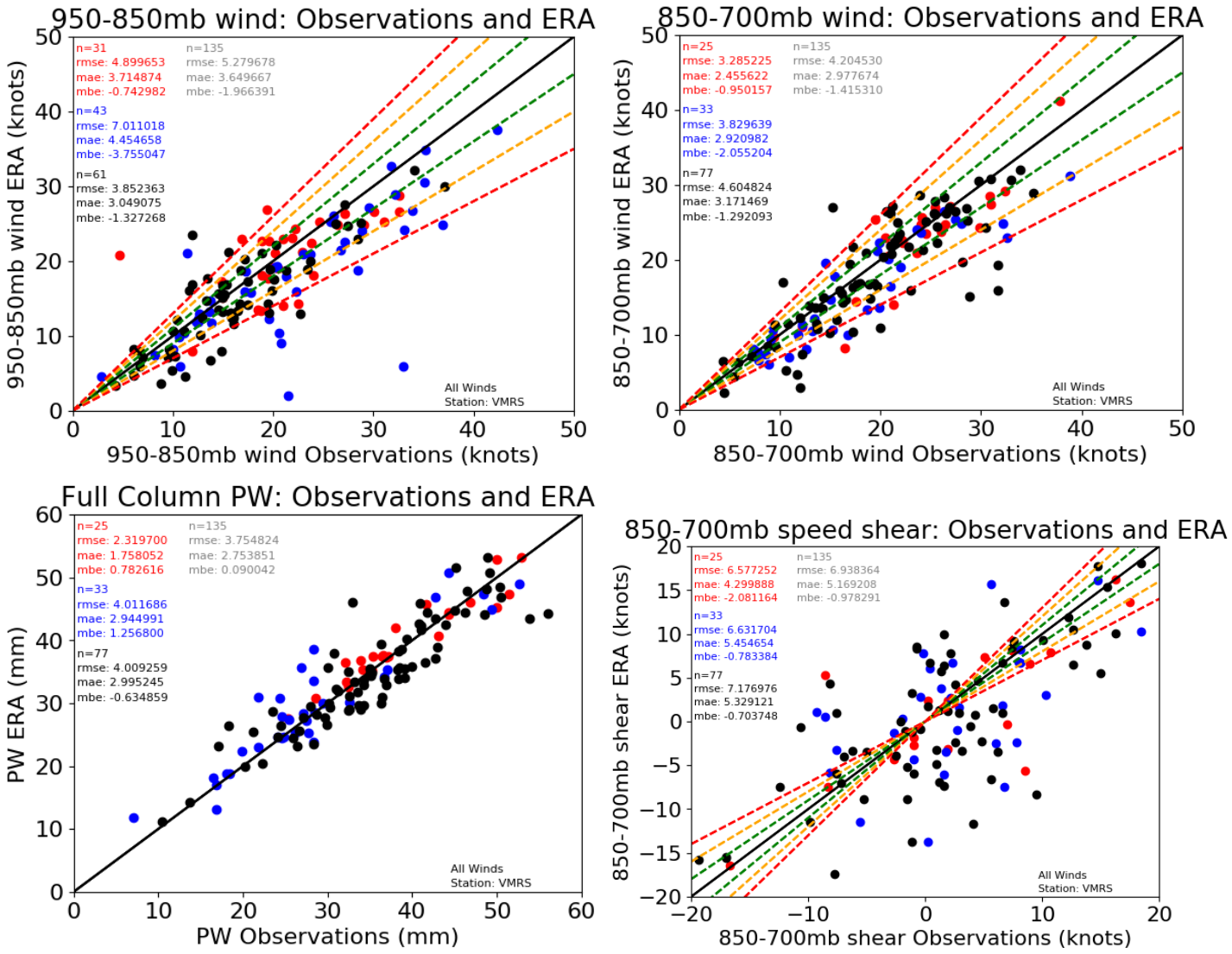

Figure A2: Same as Figure A1 but for VMRS.